

Wasserstein Gradient Flows for Moreau Envelopes of f -Divergences in Reproducing Kernel Hilbert Spaces

Viktor Stein[‡] Sebastian Neumayer[†] Nicolaj Rux[‡] Gabriele Steidl[‡]

January 17, 2025

Abstract

Commonly used f -divergences of measures, e.g., the Kullback-Leibler divergence, are subject to limitations regarding the support of the involved measures. A remedy is regularizing the f -divergence by a squared maximum mean discrepancy (MMD) associated with a characteristic kernel K . We use the kernel mean embedding to show that this regularization can be rewritten as the Moreau envelope of some function on the associated reproducing kernel Hilbert space. Then, we exploit well-known results on Moreau envelopes in Hilbert spaces to analyze the MMD-regularized f -divergences, particularly their gradients. Subsequently, we use our findings to analyze Wasserstein gradient flows of MMD-regularized f -divergences. We provide proof-of-the-concept numerical examples for flows starting from empirical measures. Here, we cover f -divergences with infinite and finite recession constants. Lastly, we extend our results to the tight variational formulation of f -divergences and numerically compare the resulting flows.

1 Introduction

In variational inference [13, 37] and generative modeling [5, 28], a common task is to minimize the f -divergence for a fixed target measure over some hypothesis space. For this, many different f -divergences were deployed in the literature, such as the Kullback-Leibler (KL) divergence [42], Tsallis- α divergences [53], power divergences [45], Jeffreys and Jensen-Shannon divergences [47], and Hellinger distances [31]. If the recession constant is infinite, then the hypothesis space in the above tasks reduces to reweighted target samples. To eliminate this disadvantage, regularized f -divergences can be applied. The probably most well-known case is the regularization of $F = \text{KL}(\cdot \mid \nu)$ with target measure ν by the squared

[‡]Institute of Mathematics, TU Berlin, Straße des 17. Juni 136, 10623 Berlin, Germany, {stein, steidl,rux}@math.tu-berlin.de

[†]Institute of Mathematics, TU Chemnitz, Reichenhainer Straße 39, 09126 Chemnitz, Germany sebastian.neumayer@mathematik.tu-chemnitz.de

Wasserstein-2 distance. This regularization appears in the backward scheme for computing the gradient flow of F in the Wasserstein geometry [38]. It can be considered as a Moreau envelope of F in the Wasserstein-2 space.

In this paper, we discuss the regularization of f -divergences by a squared maximum mean discrepancy (MMD) induced by a characteristic kernel K . Since the space of signed Borel measures embeds into the associated reproducing kernel Hilbert space (RKHS), the MMD can be rewritten as a distance in this RKHS. As our first contribution, we establish a link between our MMD-regularized f -divergences and Moreau envelopes of a specific functional on this RKHS. Here, two main challenges arise. First, covering f -divergences both with a finite and an infinite recession constant makes the analysis more involved. Second, as the kernel mean embedding is not surjective, we must suitably extend the f -divergence to the RKHS and have to prove that the corresponding functional is lower semicontinuous. Due to the established link, many of the well-known properties of Moreau envelopes also hold for our regularized f -divergences. As our second contribution, we analyze Wasserstein gradient flows of the regularized f -divergences, particularly the associated particle gradient flows. Using our theoretical insights, we prove that the regularized f -divergences are λ -convex along generalized geodesics in the Wasserstein space for sufficiently smooth kernels. Then, we show that their subdifferential consists of just one element and use this to determine the Wasserstein gradient flow equation. Finally, we deal with particle flows, which are proven to be Wasserstein gradient flows that start in an empirical measure with an empirical target measure. For the numerical simulations, we focus on the Tsallis- α divergence, which is smoothed based on the inverse multiquadric kernel. In the case of an infinite recession constant, we can apply the representer theorem to obtain a finite-dimensional problem. If the recession constant is finite, we must impose a lower bound on the regularization parameter. We simulate the gradient flows for three different target measures from the literature. Since $\alpha = 1$ corresponds to the KL divergence, we are especially interested in the behavior for different values of α . Choosing α moderately larger than one seems to improve the convergence of the gradient flow. A similar behavior was observed in [30] for another regularization.

1.1 Related work

Our work is inspired by the paper of Glaser et al. [27] (which builds on [6, 52]) on Wasserstein gradient flows with respect to the MMD-regularized KL divergence. In contrast to their paper, we deal with arbitrary f -divergences and relate the functionals to Moreau envelopes in Hilbert spaces. This helps to streamline the proofs. Moreover, our simulations cover the more general Tsallis- α divergences.

The opposite perspective is to regularize MMDs by f -divergences [41]. Their analysis covers entropy functions f with an infinite recession constant and probability measures with additional conditions for the moments. The paper focuses on kernel methods of moments as an alternative to the generalized method of moments. In contrast, we deal with gradient

flows.

Wasserstein-1 regularized f -divergences for measures on compact metric spaces are considered in [79]. When choosing their exponent α equal to two, one obtains a Moreau envelope. However, their definition of f -divergence is slightly more general than ours since it also accounts for negative measures.

The authors of [12] investigated the regularization of f -divergences using the infimal convolution with general integral probability metrics. Again, only entropy functions f with an infinite recession constant were considered. Choosing an MMD as the integral probability metric leads, in contrast to our paper, to a regularization of f -divergences with the *non-squared* MMD. For this setting, no interpretation as Moreau envelope is possible. Instead, their regularized objective can be interpreted as a Pasch-Hausdorff envelope [67, Sec. 9B] or Moreau-Yosida envelope [49, Chp. 9]. Wasserstein gradient flows of these regularized f -divergences and their discretization are discussed in [30], although neither the existence nor uniqueness of the Wasserstein gradient flow is proven.

After the submission of this work, Chen et al. published [18], which deals with the properties of $D_{f,\nu}^\lambda$ and its Wasserstein gradient flow for the Tsallis-2 entropy $f := (\cdot - 1)^2$. Due to the simple structure of f , they can derive a closed-form expression for the minimization problem defining $D_{f,\nu}^\lambda$ and show that this expression is equal to $d_{\tilde{K}}^2$ for a modified kernel \tilde{K} .

1.2 Outline of the paper

In Section 2, we collect basic facts from convex analysis, especially about Moreau envelopes. Further, we recall the notation of RHKSs and MMDs. Then, in Section 3, we discuss f -divergences both with finite and an infinite recession constant. We introduce their MMD-regularized counterparts and establish the relation to Moreau envelopes of a specific proper, convex, and lower semicontinuous function on the RKHS associated with the kernel of the MMD. In Section 4, we recall the concept of Wasserstein gradient flow and prove the existence and uniqueness of the Wasserstein gradient flow with respect to MMD-regularized f -divergences. We discuss the simulation of these Wasserstein gradient flows when both the target and the starting point of the flow are empirical measures in Section 5. Here, we show that the representer theorem can also be applied for the case of f -divergences with finite recession constant. Then, we illustrate the behavior of such flows with three numerical examples in Section 6. Finally, we conclude in Section 7. We collect examples of entropy functions, their conjugates, and their associated f -divergences in Appendix A. Further, we discuss regularizing the tight variational formulations of f -divergences in Appendix B. Details for the duality gaps are added in Appendix C. Further ablation plots and implementation details are provided in the supplementary material included in the arXiv version (<https://arxiv.org/abs/2402.04613>).

2 Convex Analysis in Reproducing Kernel Hilbert spaces

This section contains the necessary preliminaries and notions. In Subsection 2.1, we start with basic facts from convex analysis in Hilbert spaces, especially Moreau envelopes and proximal mappings, which can be found, e.g., in the textbook [7]. Our Hilbert spaces of choice will be RKHSs, which are properly introduced in Subsection 2.2. In particular, we require their relation to the space of signed Borel measures in terms of the so-called kernel mean embedding. This embedding also relates the distance in RKHSs with the MMD of measures.

2.1 Moreau Envelopes in Hilbert Spaces

Let \mathcal{H} be a *Hilbert* space with inner product $\langle \cdot, \cdot \rangle_{\mathcal{H}}$ and corresponding norm $\| \cdot \|_{\mathcal{H}}$. The domain of an extended function $F: \mathcal{H} \rightarrow (-\infty, \infty]$ is defined by $\text{dom}(F) := \{h \in \mathcal{H} : F(h) < \infty\}$, and F is proper if $\text{dom}(F) \neq \emptyset$. By $\Gamma_0(\mathcal{H})$, we denote the set of proper, convex, lower semicontinuous extended real-valued functions on \mathcal{H} . The *Fenchel conjugate function* of a proper function $F: \mathcal{H} \rightarrow (-\infty, \infty]$ is given by

$$F^*(h) = \sup_{g \in \mathcal{H}} \{\langle h, g \rangle_{\mathcal{H}} - F(g)\}.$$

The conjugate F^* is convex and lower semicontinuous. The *subdifferential* of a function $F \in \Gamma_0(\mathcal{H})$ at $h \in \text{dom}(F)$ is defined as the set

$$\partial F(h) := \{p \in \mathcal{H} : F(g) \geq F(h) + \langle p, g - h \rangle_{\mathcal{H}} \forall g \in \mathcal{H}\}.$$

If F is differentiable at h , then $\partial F(h) = \{\nabla F(h)\}$. Further, $p \in \partial F(h)$ implies $h \in \partial F^*(p)$.

Next, recall that the *Moreau envelope* of a function $G \in \Gamma_0(\mathcal{H})$ is defined by

$$G^\lambda(h) := \min_{g \in \mathcal{H}} \left\{ G(g) + \frac{1}{2\lambda} \|h - g\|_{\mathcal{H}}^2 \right\}, \quad \lambda > 0, \quad (1)$$

where the minimizer is unique. Hence, the *proximal map* $\text{prox}_{\lambda G}: \mathcal{H} \rightarrow \mathcal{H}$ with

$$\text{prox}_{\lambda G}(h) := \arg \min_{g \in \mathcal{H}} \left\{ G(g) + \frac{1}{2\lambda} \|h - g\|_{\mathcal{H}}^2 \right\}, \quad \lambda > 0,$$

is well-defined. The Moreau envelope has the following advantageous properties.

Theorem 1. *The Moreau envelope of $G \in \Gamma_0(\mathcal{H})$ has the following properties:*

i) The dual formulation of $G^\lambda: \mathcal{H} \rightarrow \mathbb{R}$ reads as

$$G^\lambda(h) = \max_{p \in \mathcal{H}} \left\{ \langle h, p \rangle_{\mathcal{H}} - G^*(p) - \frac{\lambda}{2} \|p\|_{\mathcal{H}}^2 \right\}. \quad (2)$$

If \hat{p} maximizes (2), then $\hat{g} = h - \lambda \hat{p}$ minimizes (1) and vice versa.

ii) The function G^λ is Fréchet differentiable with derivative given by

$$\nabla G^\lambda(h) = \lambda^{-1}(h - \text{prox}_{\lambda G}(h)).$$

In particular, it holds that ∇G^λ is $\frac{1}{\lambda}$ -Lipschitz and that G^λ is continuous.

iii) For $\lambda \searrow 0$, we have $G^\lambda \nearrow G$, and for $\lambda \rightarrow \infty$ that $G^\lambda \searrow \inf_{x \in \mathbb{R}^d} \{G(x)\}$ pointwise.

2.2 Reproducing Kernel Hilbert Spaces and MMDs

A Hilbert space \mathcal{H} of real-valued functions on \mathbb{R}^d is called a *reproducing kernel Hilbert space* (RKHS), if the point evaluations $h \mapsto h(x)$, $h \in \mathcal{H}$, are continuous for all $x \in \mathbb{R}^d$. There exist various textbooks on RKHS from different points of view, see, e.g., [76, 24, 72, 88]. By [76, Thm. 4.20], every RKHS admits a unique symmetric, positive definite function $K: \mathbb{R}^d \times \mathbb{R}^d \rightarrow \mathbb{R}$ which is determined by the reproducing property

$$h(x) = \langle h, K(x, \cdot) \rangle_{\mathcal{H}} \quad \text{for all } h \in \mathcal{H}. \quad (3)$$

In particular, we have that $K(x, \cdot) \in \mathcal{H}$ for all $x \in \mathbb{R}^d$. Conversely, for any symmetric, positive definite function $K: \mathbb{R}^d \times \mathbb{R}^d \rightarrow \mathbb{R}$, there exists a unique RKHS with reproducing kernel K , denoted by \mathcal{H}_K [76, Thm. 4.21].

Assumption 1. In the following, we use the term „kernel” for symmetric, positive definite functions $K: \mathbb{R}^d \times \mathbb{R}^d \rightarrow \mathbb{R}$ that are

- i) bounded, i.e., $\sup_{x \in \mathbb{R}^d} K(x, x) < \infty$, and fulfil
- ii) $K(x, \cdot) \in \mathcal{C}_0(\mathbb{R}^d)$ for all $x \in \mathbb{R}^d$.

The properties (i) and (ii) are equivalent to the fact that $\mathcal{H}_K \subset \mathcal{C}_0(\mathbb{R}^d)$. Further, the embedding is continuous: $\mathcal{H}_K \hookrightarrow \mathcal{C}_0(\mathbb{R}^d)$ [73, Cor. 3].

RKHSs are closely related to the Banach space $\mathcal{M}(\mathbb{R}^d)$ of finite signed Borel measures equipped with total variation norm $\|\cdot\|_{\text{TV}}$. Later, we also need its subset $\mathcal{M}_+(\mathbb{R}^d)$ of non-negative measures. For any $\mu \in \mathcal{M}(\mathbb{R}^d)$, there exists a unique $m_\mu \in \mathcal{H}_K$ with

$$\begin{aligned} \mathbb{E}_\mu[h] &:= \langle h, \mu \rangle_{\mathcal{C}_0 \times \mathcal{M}} = \int_{\mathbb{R}^d} h(x) \, d\mu(x) = \int_{\mathbb{R}^d} \langle h, K(x, \cdot) \rangle_{\mathcal{H}_K} \, d\mu(x) \\ &= \left\langle h, \int_{\mathbb{R}^d} K(x, \cdot) \, d\mu(x) \right\rangle_{\mathcal{H}_K} = \langle h, m_\mu \rangle_{\mathcal{H}_K} \end{aligned} \quad (4)$$

for all $h \in \mathcal{H}_K$. The linear, bounded mapping $m: \mathcal{M}(\mathbb{R}^d) \rightarrow \mathcal{H}_K$ with $\mu \mapsto m_\mu$ given by

$$m_\mu(x) = \langle K(x, \cdot), \mu \rangle = \int_{\mathbb{R}^d} K(x, y) \, d\mu(y), \quad (5)$$

is called *kernel mean embedding* (KME) [50, Sec. 3.1].

Assumption 2. In this paper, we restrict our attention to so-called *characteristic kernels* K , for which the KME is injective.

A kernel K is characteristic if and only if \mathcal{H}_K is dense in $(\mathcal{C}_0(\mathbb{R}^d), \|\cdot\|_\infty)$, see [73]. The KME is not surjective and we only have $\overline{(\text{ran}(m), \|\cdot\|_{\mathcal{H}_K})} = \mathcal{H}_K$, see [77].

The *maximum mean discrepancy* (MMD) [15, 29] $d_K: \mathcal{M}(\mathbb{R}^d) \times \mathcal{M}(\mathbb{R}^d) \rightarrow \mathbb{R}$ is defined as

$$\begin{aligned} d_K(\mu, \nu)^2 &:= \int_{\mathbb{R}^d \times \mathbb{R}^d} K(x, y) \, d(\mu(x) - \nu(x)) \, d(\mu(y) - \nu(y)) \\ &= \int_{\mathbb{R}^d \times \mathbb{R}^d} K(x, y) \, d\mu(x) \, d\mu(y) - 2 \int_{\mathbb{R}^d \times \mathbb{R}^d} K(x, y) \, d\mu(x) \, d\nu(y) \\ &\quad + \int_{\mathbb{R}^d \times \mathbb{R}^d} K(x, y) \, d\nu(x) \, d\nu(y). \end{aligned} \tag{6}$$

By the reproducing property (3), see [29, Lemma 4], (6) can be rewritten as

$$d_K(\mu, \nu) = \|m_\mu - m_\nu\|_{\mathcal{H}_K}.$$

Since the KME is injective, d_K is a metric on $\mathcal{M}(\mathbb{R}^d)$ and, in particular, $d_K(\mu, \nu) = 0$ if and only if $\mu = \nu$. The widely used *radial kernels* are of the form $K(x, y) = \phi(\|x - y\|_2^2)$ for some continuous function $\phi: [0, \infty) \rightarrow \mathbb{R}$.

Remark 2. By Schoenberg's theorem [85, Thm. 7.13], a radial kernel K is positive definite if and only if ϕ is completely monotone on $[0, \infty)$, that is $\phi \in \mathcal{C}^\infty((0, \infty)) \cap \mathcal{C}([0, \infty))$ and $(-1)^k \phi^{(k)}(r) \geq 0$ for all $k \in \mathbb{N}$ and all $r > 0$. Hence, ϕ and ϕ'' are decreasing on $(0, \infty)$. Moreover, the Hausdorff–Bernstein–Widder theorem [85, Thm. 7.11] asserts that ϕ is completely monotone on $[0, \infty)$ if and only if there exists a non-negative finite Borel measure ν on $\mathcal{B}([0, \infty))$ such that

$$\phi(r) = \int_0^\infty e^{-rt} \, d\nu(t), \quad \forall r \geq 0.$$

By [75, Prop. 11], $K(x, y) = \phi(\|x - y\|_2^2)$ is characteristic if and only if $\text{supp}(\nu) \neq \{0\}$. Examples of radial characteristic kernels are the Gaussians with $\phi(r) = \exp(-\frac{1}{2\sigma^2}r)$, $\sigma \in \mathbb{R}$ and the inverse multiquadric with $\phi(r) = (\sigma + r)^{-\frac{1}{2}}$, $\sigma > 0$.

We have the following regularity result, where both $\phi'(0)$ and $\phi''(0)$ denote the one-sided derivatives.

Lemma 3. For a radial kernel $K(x, y) = \phi(\|x - y\|_2^2)$ with $\phi \in \mathcal{C}^2([0, \infty))$ it holds that $\mathcal{H}_K \hookrightarrow C^2(\mathbb{R}^d)$. Then, we have for any $y, \tilde{y} \in \mathbb{R}^d$ and all $i \in \{1, \dots, d\}$ that

$$\|\partial_{y_i} K(\cdot, y)\|_{\mathcal{H}_K}^2 = -2\phi'(0)$$

and

$$\|\partial_{y_i} K(\cdot, y) - \partial_{\tilde{y}_i} K(\cdot, \tilde{y})\|_{\mathcal{H}_K}^2 \leq 4\phi''(0) (2|y_i - \tilde{y}_i|^2 + \|y - \tilde{y}\|_2^2).$$

Furthermore, we have for any $h \in \mathcal{H}_K$ that

$$\|\nabla h(y) - \nabla h(\tilde{y})\|_2 \leq 2\|h\|_{\mathcal{H}_K} \sqrt{\phi''(0)(d+2)} \|y - \tilde{y}\|_2. \quad (7)$$

Proof. The continuity of the embedding follows from [76, Cor. 4.36]. Next, for $x, y \in \mathbb{R}^d$ we directly compute $\partial_{x_i} \partial_{y_i} K(x, y) = -4\phi''(\|x - y\|_2^2)(x_i - y_i)^2 - 2\phi'(\|x - y\|_2^2)$. By applying [76, Lem. 4.34] for the feature map $y \mapsto K(\cdot, y)$, we get

$$\langle \partial_{y_i} K(\cdot, y), \partial_{\tilde{y}_i} K(\cdot, \tilde{y}) \rangle_{\mathcal{H}_K} = \partial_{y_i} \partial_{\tilde{y}_i} K(y, \tilde{y}) = -4\phi''(\|y - \tilde{y}\|_2^2)(y_i - \tilde{y}_i)^2 - 2\phi'(\|y - \tilde{y}\|_2^2) \quad (8)$$

and in particular $\|\partial_{y_i} K(\cdot, y)\|_{\mathcal{H}_K}^2 = -2\phi'(0)$. By (8) and since ϕ' is Lipschitz continuous with Lipschitz constant $\|\phi''\|_\infty = \phi''(0)$, see Remark 2, it holds

$$\begin{aligned} \|\partial_{y_i} K(\cdot, y) - \partial_{\tilde{y}_i} K(\cdot, \tilde{y})\|_{\mathcal{H}_K}^2 &= -4\phi'(0) + 8\phi''(\|y - \tilde{y}\|_2^2)(y_i - \tilde{y}_i)^2 + 4\phi'(\|y - \tilde{y}\|_2^2) \\ &\leq 4\phi''(0) (2(y_i - \tilde{y}_i)^2 + \|y - \tilde{y}\|_2^2). \end{aligned}$$

The final assertion follows by

$$\begin{aligned} |\partial_{y_i} h(y) - \partial_{\tilde{y}_i} h(\tilde{y})| &= |\partial_i \langle h, K(\cdot, y) \rangle_{\mathcal{H}_K} - \partial_i \langle h, K(\cdot, \tilde{y}) \rangle_{\mathcal{H}_K}| \\ &= |\langle h, \partial_{y_i} K(\cdot, y) - \partial_{y_i} K(\cdot, \tilde{y}) \rangle_{\mathcal{H}_K}| \\ &\leq \|h\|_{\mathcal{H}_K} \|\partial_{y_i} K(\cdot, y) - \partial_{y_i} K(\cdot, \tilde{y})\|_{\mathcal{H}_K}. \end{aligned}$$

This finishes the proof. \square

In the rest of this paper, kernels always have to fulfill Assumptions 1 and 2.

3 MMD-regularized f -Divergences and Moreau Envelopes

Let us briefly describe the path of this section. First, we define f -divergences D_f of non-negative measures for entropy functions f with infinite or finite recession constant. Such f -divergences were first introduced by [22, 2], and we refer to [46] for a detailed overview. We prove some of their properties in Subsection 3.1, where allowing a finite recession constant makes the proofs more expansive. Then, in Subsection 3.2, we deal with the associated functionals $D_{f,\nu} := D_f(\cdot|\nu)$ with a fixed target measure ν . If the recession constant is infinite, then $D_{f,\nu}$ is only finite for measures that are absolutely continuous with respect to ν . This disadvantage can be circumvented by using the MMD-regularized functional

$$D_{f,\nu}^\lambda(\mu) := \inf_{\sigma \in \mathcal{M}_+(\mathbb{R}^d)} \left\{ D_{f,\nu}(\sigma) + \frac{1}{2\lambda} \underbrace{d_K(\mu, \sigma)^2}_{\|m_\mu - m_\sigma\|_{\mathcal{H}_K}^2} \right\}, \quad \lambda > 0. \quad (9)$$

A different form of MMD-regularized f -divergences, where $\mu, \nu \in \mathcal{P}(\mathbb{R}^d)$ and the infimum in (9) is only taken over $\mathcal{P}(\mathbb{R}^d)$, is discussed in Appendix B.

Now, our main goal is to show that (9) can be rewritten as the concatenation of the Moreau envelope of some $G_{f,\nu}: \mathcal{H}_K \rightarrow (-\infty, \infty]$, and the KME. To this end, we introduce $G_{f,\nu} = D_{f,\nu} \circ m^{-1}$ on $\text{ran}(m)$ and set $G_{f,\nu} = \infty$ otherwise. This function is proper and convex. We prove that $G_{f,\nu}$ is lower semicontinuous, where we have to face the difficulty that $\text{ran}(m) \neq \mathcal{H}_K$. Then $G_{f,\nu} \in \Gamma_0(\mathcal{H}_K)$ yields the desired Moreau envelope identification

$$D_{f,\nu}^\lambda(\mu) = G_{f,\nu}^\lambda(m_\mu) := \min_{g \in \mathcal{H}_K} \left\{ G_{f,\nu}(g) + \frac{1}{2\lambda} \|g - m_\nu\|_{\mathcal{H}_K}^2 \right\}.$$

which allows to exploit Theorem 1 to show various of its properties in Subsection 3.3.

3.1 f -Divergences

A function $f: \mathbb{R} \rightarrow [0, \infty]$ is called an *entropy function* if $f \in \Gamma_0(\mathbb{R})$ with $f(t) = \infty$ for $t < 0$ and $f(1) = 0$. Its *recession constant* is given by $f'_\infty = \lim_{t \rightarrow \infty} \frac{f(t)}{t}$. Then, $f^* \in \Gamma_0(\mathbb{R})$ is non-decreasing and $\text{int}(\text{dom}(f^*)) = (-\infty, f'_\infty)$, see, e.g., [45]. Further, f^* is continuous on $\text{dom}(f^*)$ and $f^*(0) = 0$, in particular $0 \in \text{dom}(f^*)$. By definition of the subdifferential and since $f(1) = 0$, it follows that $0 \in \partial f(1)$ and thus $1 \in \partial f^*(0)$. Several entropy functions with their recession constants and conjugate functions are collected in Table 1 in Appendix A.

Let f be an entropy function and $\nu \in \mathcal{M}_+(\mathbb{R}^d)$. Recall that every measure $\mu \in \mathcal{M}_+(\mathbb{R}^d)$ admits a *unique Lebesgue decomposition* $\mu = \rho\nu + \mu^s$, where $\rho \in L^1(\mathbb{R}^d, \nu)$, $\rho \geq 0$ and $\mu^s \perp \nu$, i.e., there exists a Borel set $\mathcal{A} \subseteq \mathbb{R}^d$ such that $\nu(\mathbb{R}^d \setminus \mathcal{A}) = 0$ and $\mu^s(\mathcal{A}) = 0$ [45, Lemma 2.3]. The f -divergence $D_f: \mathcal{M}_+(\mathbb{R}^d) \times \mathcal{M}_+(\mathbb{R}^d) \rightarrow [0, \infty]$ between a measure $\mu = \rho\nu + \mu^s \in \mathcal{M}_+(\mathbb{R}^d)$ and $\nu \in \mathcal{M}_+(\mathbb{R}^d)$ is defined by

$$D_f(\rho\nu + \mu^s \mid \nu) = \int_{\mathbb{R}^d} f \circ \rho \, d\nu + f'_\infty \mu^s(\mathbb{R}^d) = \sup_{\substack{g \in \mathcal{C}_b(\mathbb{R}^d), \\ f^* \circ g \in \mathcal{C}_b(\mathbb{R}^d)}} \left\{ \int_{\mathbb{R}^d} g \, d\mu - \int_{\mathbb{R}^d} f^* \circ g \, d\nu \right\} \quad (10)$$

with the usual convention $0 \cdot (\pm\infty) = 0$, see [45, Eq. (2.35), Thm. 2.7, Rem. 2.8]. The function D_f is jointly convex and non-negative, see [45, Cor. 2.9]. Moreover, we will need the following lemma.

Lemma 4. *Let $f \in \Gamma_0(\mathbb{R})$ be an entropy function with the unique minimizer 1.*

- i) *Divergence: For $\mu, \nu \in \mathcal{M}_+(\mathbb{R}^d)$, the relation $D_f(\mu, \nu) = 0$ implies that $\mu = \nu$.*
- ii) *We have $f'_\infty > 0$ and thus $\lim_{t \rightarrow \infty} f(t) = \infty$.*

Proof. i) Suppose we have $\nu \in \mathcal{M}_+(\mathbb{R}^d)$ and $\mu = \rho\nu + \mu^s \in \mathcal{M}_+(\mathbb{R}^d)$ such that $D_f(\mu \mid \nu) = 0$. Since both summands in the primal definition (10) of D_f are non-negative,

they must be equal to zero. In particular, $\mu^s(\mathbb{R}^d) = 0$ and since $\mu^s \in \mathcal{M}_+(\mathbb{R}^d)$, this implies $\mu^s = 0$. Hence, $\mu = \rho\nu$ and

$$D_f(\mu | \nu) = D_f(\rho\nu | \nu) = \int_{\mathbb{R}^d} (f \circ \rho)(x) d\nu(x) = 0.$$

Since f is non-negative and $\nu \in \mathcal{M}_+(\mathbb{R}^d)$, we must have $f \circ \rho = 0$ ν -a.e. Since $f(1) = 0$ is the unique minimum, this implies $\rho = 1$ ν -a.e., namely that $\mu = \nu$.

- ii) Fix $\tau > 1$. For any $t > \tau$ we write τ as $\tau = 1 - \lambda + \lambda t$, with $\lambda = \frac{\tau-1}{t-1} \in (0, 1)$. By the convexity of f we have

$$0 < f(\tau) \leq (1 - \lambda)f(1) + \lambda f(t) = \lambda f(t) = \frac{\tau - 1}{t - 1} f(t). \quad (11)$$

Since 1 is the unique minimizer and $\tau > 1$, (11) implies

$$f'_\infty = \lim_{t \rightarrow \infty} \frac{f(t)}{t} = \lim_{t \rightarrow \infty} \frac{f(t)}{t-1} \geq \frac{f(\tau)}{\tau-1} > 0.$$

Immediately, $f'_\infty > 0$ yields $\lim_{t \rightarrow \infty} f(t) = \infty$. □

Assumption 3. From now on, we assume that all entropy functions fulfill the assumption in Lemma 4, that is, the minimizer in 1 is unique.

Examples of f -divergences are contained in Table 2 in Appendix A. Assumption 3 is fulfilled for all f -divergences in Table 1 except for the Marton divergence, the hockey stick divergence, and the trivial zero divergence. However, it is not hard to check that the Marton divergence and the hockey stick divergence are positive definite on the space of *probability* measures, $\mathcal{P}(\mathbb{R}^d)$, too. Below is an example of a non-trivial f -divergence that does not have this property.

Example 5 (Rescaled Marton divergence). Let $f(t) = \max(\frac{1}{2} - t, 0)^2$ on $[0, \infty)$. Then $f'_\infty = 0$ and we have for any absolutely continuous $\nu \in \mathcal{P}(\mathbb{R}^d)$ that $D_f(\frac{1}{2}\nu + \frac{1}{2}\delta_0 | \nu) = f(\frac{1}{2}) = 0$.

Recall that $\mathcal{M}(\mathbb{R}^d)$ is the dual space of $\mathcal{C}_0(\mathbb{R}^d)$. A sequence of measures $(\mu_n)_n \subset \mathcal{M}(\mathbb{R}^d)$ converges weak* to a measure $\mu \in \mathcal{M}(\mathbb{R}^d)$ if we have for all $g \in \mathcal{C}_0(\mathbb{R}^d)$ that $\langle g, \mu_n \rangle \rightarrow \langle g, \mu \rangle$ as $n \rightarrow \infty$. Moreover, if $(\mu_n)_n \subset \mathcal{M}_+(\mathbb{R}^d)$ is bounded, then $\mu \in \mathcal{M}_+(\mathbb{R}^d)$, see [61, Lemma 4.71, Cor. 4.74].

The following lemma also follows from the more general [3, Thm. 2.34], but we prefer to give a simpler proof for our setting to make the paper self-contained.

Lemma 6. For any fixed $\nu \in \mathcal{M}_+(\mathbb{R}^d)$, the f -divergence (10) can be rewritten as

$$D_f(\rho\nu + \mu^s \mid \nu) = \sup_{g \in \mathcal{C}_0(\mathbb{R}^d; \text{dom}(f^*))} \left\{ \int_{\mathbb{R}^d} g \, d\mu - \int_{\mathbb{R}^d} f^* \circ g \, d\nu \right\}. \quad (12)$$

Therefore, D_f is jointly weak* lower semicontinuous.

Proof. In the proof, we must be careful concerning the support of ν .

- i) (10) \geq (12): This direction is obvious since $g \in \mathcal{C}_0(\mathbb{R}^d; \text{dom}(f^*))$, $0 \in \text{dom}(f^*)$ and the continuity of f^* on its domain imply $g \in \mathcal{C}_b(\mathbb{R}^d)$ and $f^* \circ g \in \mathcal{C}_b(\mathbb{R}^d)$.
- ii) (10) \leq (12): Let $g \in \mathcal{C}_b(\mathbb{R}^d)$ with $f^* \circ g \in \mathcal{C}_b(\mathbb{R}^d)$. Using continuous cutoff functions, we can approximate g by a family of functions $(g_k)_{k \in \mathbb{N}} \subset \mathcal{C}_0(\mathbb{R}^d; \text{dom}(f^*))$ with $\sup g \geq \max g_k \geq \inf g_k \geq \min(\inf g, 0)$, which implies $|f^* \circ g_k| \leq \sup |f^* \circ g|$, for any $k \in \mathbb{N}$, and $\lim_{k \rightarrow \infty} g_k(x) = g(x)$ for all $x \in \mathbb{R}^d$. Further, the continuity of f^* on its domain implies that $(f^* \circ g_k)_{k \in \mathbb{N}}$ satisfies $\lim_{k \rightarrow \infty} (f^* \circ g_k)(x) = (f^* \circ g)(x)$. Now, the claim follows as in the first part using the dominated convergence theorem.
- iii) Let $(\mu_n)_n$ and $(\nu_n)_n$ converge weak* to μ and ν , respectively. Since f^* is continuous on its domain, where $f^*(0) = 0$ and $g \in \mathcal{C}_0(\mathbb{R}^d; \text{dom}(f^*))$, it follows that $f^* \circ g \in \mathcal{C}_0(\mathbb{R}^d)$. Then, we have for $g \in \mathcal{C}_0(\mathbb{R}^d; \text{dom}(f^*))$ that

$$\lim_{n \rightarrow \infty} \{ \langle g, \mu_n \rangle - \langle f^* \circ g, \nu_n \rangle \} = \langle g, \mu \rangle - \langle f^* \circ g, \nu \rangle \quad (13)$$

and by inserting (13) into (12) we get

$$\begin{aligned} D_f(\mu \mid \nu) &= \sup_{g \in \mathcal{C}_0(\mathbb{R}^d; \text{dom}(f^*))} \left\{ \lim_{n \rightarrow \infty} \langle g, \mu_n \rangle - \langle f^* \circ g, \nu_n \rangle \right\} \\ &\leq \liminf_{n \rightarrow \infty} \sup_{g \in \mathcal{C}_0(\mathbb{R}^d; \text{dom}(f^*))} \left\{ \langle g, \mu_n \rangle - \langle f^* \circ g, \nu_n \rangle \right\} = \liminf_{n \rightarrow \infty} D_f(\mu_n \mid \nu_n). \end{aligned}$$

Thus, D_f is jointly weak* lower semicontinuous. \square

3.2 Regularized f -Divergences

To overcome the drawback that $D_f(\mu, \nu)$ requires μ to be absolutely continuous with respect to ν if $f'_\infty = \infty$, we introduce the MMD-regularized f -divergence $D_f^\lambda: \mathcal{M}_+(\mathbb{R}^d) \times \mathcal{M}_+(\mathbb{R}^d) \rightarrow [0, \infty)$ as

$$D_f^\lambda(\mu \mid \nu) := \inf_{\sigma \in \mathcal{M}_+(\mathbb{R}^d)} \left\{ D_f(\sigma \mid \nu) + \frac{1}{2\lambda} d_K(\mu, \sigma)^2 \right\}, \quad \lambda > 0. \quad (14)$$

For fixed $\nu \in \mathcal{M}_+(\mathbb{R}^d)$, we investigate the functional $D_{f,\nu} := D_f(\cdot \mid \nu): \mathcal{M}(\mathbb{R}^d) \rightarrow [0, \infty]$, set to ∞ on $\mathcal{M}(\mathbb{R}^d) \setminus \mathcal{M}_+(\mathbb{R}^d)$. Similarly, we consider its regularized version $D_{f,\nu}^\lambda: \mathcal{M}(\mathbb{R}^d) \rightarrow$

$[0, \infty)$ that was announced in (9). Note that $D_{f,\nu}^\lambda$ is well-defined also for nonpositive measures. Moreover, we always have $D_{f,\nu}^\lambda(\mu) < \infty$.

Now, we aim to reformulate (9) as the Moreau envelope of a certain function on \mathcal{H}_K . Using the KME in (5), we see that

$$D_{f,\nu}(\mu) = G_{f,\nu}(m_\mu), \quad (15)$$

where $G_{f,\nu}: \mathcal{H}_K \rightarrow [0, \infty]$ is given by

$$G_{f,\nu}(h) := \begin{cases} D_{f,\nu}(\mu), & \text{if } \exists \mu \in \mathcal{M}_+(\mathbb{R}^d) \text{ s.t. } h = m_\mu, \\ \infty, & \text{else.} \end{cases} \quad (16)$$

Since m^{-1} is linear on $\text{ran}(m)$ and D_f is jointly convex, the concatenation $G_{f,\nu}$ is convex. Further, $G_{f,\nu}(m_\nu) = 0$, so that $G_{f,\nu}$ is also proper.

We now prove that although $\text{ran}(m)$ is not closed in \mathcal{H}_K , the function $G_{f,\nu}$ is lower semicontinuous. Hence, the theory for Moreau envelopes on $\Gamma_0(\mathcal{H}_K)$ applies.

Lemma 7. *The function $G_{f,\nu}: \mathcal{H}_K \rightarrow [0, \infty]$ is lower semicontinuous.*

Proof. Fix $h \in \mathcal{H}_K$ and let $(h_n)_n \subset \mathcal{H}_K$ with $h_n \rightarrow h$. We need to show that $G_{f,\nu}(h) \leq \liminf_{n \rightarrow \infty} G_{f,\nu}(h_n)$. If $\liminf_{n \rightarrow \infty} G_{f,\nu}(h_n) = +\infty$, we are done. For $\liminf_{n \rightarrow \infty} G_{f,\nu}(h_n) < +\infty$, we pass to a subsequence which realizes the limes inferior. We choose this subsequence such that $G_{f,\nu}(h_n) < \infty$ for all $n \in \mathbb{N}$. Then, there exist $\mu_n \in \mathcal{M}_+(\mathbb{R}^d)$ with $m_{\mu_n} = h_n$. In principle, two cases can occur.

Case 1: *The sequence $(\|\mu_n\|_{\text{TV}})_n$ diverges to ∞ .*

Since $D_{f,0} = f'_\infty \cdot \|\cdot\|_{\text{TV}}$, this is impossible for $\nu = 0$. If $\nu \in \mathcal{M}_+(\mathbb{R}^d) \setminus \{0\}$, then Jensen's inequality implies

$$\begin{aligned} G_{f,\nu}(h_n) &= D_{f,\nu}(\mu_n) = \int_{\mathbb{R}^d} f \circ \rho_n \, d\nu + f'_\infty \mu_n^s(\mathbb{R}^d) \\ &\geq \|\nu\|_{\text{TV}} f \left(\int_{\mathbb{R}^d} \frac{\rho_n}{\|\nu\|_{\text{TV}}} \, d\nu \right) + f'_\infty \mu_n^s(\mathbb{R}^d) \\ &= \|\nu\|_{\text{TV}} f \left(\frac{1}{\|\nu\|_{\text{TV}}} \left(\mu_n(\mathbb{R}^d) - \mu_n^s(\mathbb{R}^d) \right) \right) + f'_\infty \mu_n^s(\mathbb{R}^d). \end{aligned} \quad (17)$$

Since $\lim_{n \rightarrow \infty} G_{f,\nu}(h_n) < \infty$ and $f'_\infty > 0$, (17) implies that the sequence $(\mu_n^s(\mathbb{R}^d))_n$ must be bounded. By Lemma 4 the same holds for the sequence $(\mu_n(\mathbb{R}^d) - \mu_n^s(\mathbb{R}^d))_n$. Hence, also $(\mu_n(\mathbb{R}^d))_n = (\|\mu_n\|_{\text{TV}})_n$ is bounded, which contradicts our initial assumption and thus this case cannot occur.

Case 2: *The sequence $(\mu_n)_n$ satisfies $\liminf_{n \rightarrow \infty} \|\mu_n\|_{\text{TV}} < \infty$.*

Since $\mathcal{C}_0(\mathbb{R}^d)$ is separable and $\mathcal{C}_0(\mathbb{R}^d)^* \cong \mathcal{M}(\mathbb{R}^d)$, the Banach-Alaoglu theorem [40, Cor. 5.4.2]

implies that there exists a subsequence $(\mu_{n_k})_k$ which converges weak* to some $\mu \in \mathcal{M}(\mathbb{R}^d)$. Since $K(x, \cdot) \in \mathcal{C}_0(\mathbb{R}^d)$ for any $x \in \mathbb{R}^d$, we thus have

$$\lim_{k \rightarrow \infty} m_{\mu_{n_k}}(x) = \lim_{k \rightarrow \infty} \int_{\mathbb{R}^d} K(x, y) d\mu_{n_k}(y) = \int_{\mathbb{R}^d} K(x, y) d\mu(y) = m_\mu(x). \quad (18)$$

Since $(m_{\mu_{n_k}})_k$ converges to h in \mathcal{H}_K , (18) entails

$$h(x) = \lim_{k \rightarrow \infty} m_{\mu_{n_k}}(x) = m_\mu(x) \quad \forall x \in \mathbb{R}^d.$$

Thus, h is represented by the measure μ . Furthermore, $\mu \in \mathcal{M}_+(\mathbb{R}^d)$ as $(\mu_n)_n$ is bounded. The weak* lower semicontinuity of $D_{f,\nu}$ from Lemma 6 yields

$$G_{f,\nu}(h) = D_{f,\nu}(\mu) \leq \liminf_{k \rightarrow \infty} D_{f,\nu}(\mu_{n_k}) = \liminf_{k \rightarrow \infty} G_{f,\nu}(h_{n_k}) = \lim_{n \rightarrow \infty} G_{f,\nu}(h_n).$$

□

The following lemma and its proof build upon the theory of convex integral functionals initiated by [65, 66] and developed in, e.g., [16].

Lemma 8. *The conjugate function of $G_{f,\nu}$ in (16) is given by*

$$G_{f,\nu}^*(h) = \mathbb{E}_\nu[f^* \circ h] + \iota_{\mathcal{C}_0(\mathbb{R}^d, \overline{\text{dom}(f^*)}}(h) \quad (19)$$

Proof. Using (4) and (15), we obtain for $h \in \mathcal{H}_K$ that

$$\begin{aligned} G_{f,\nu}^*(h) &= \sup_{g \in \mathcal{H}_K} \{ \langle g, h \rangle_{\mathcal{H}_K} - G_{f,\nu}(g) \} = \sup_{\mu \in \mathcal{M}_+(\mathbb{R}^d)} \{ \langle m_\mu, h \rangle_{\mathcal{H}_K} - D_{f,\nu}(\mu) \} \\ &= \sup_{\mu \in \mathcal{M}_+(\mathbb{R}^d)} \{ \langle h, \mu \rangle_{\mathcal{C}_0 \times \mathcal{M}} - D_{f,\nu}(\mu) \}. \end{aligned}$$

Applying [1, Prop. 24] (a similar argument can be found in the earlier paper [60]) with (in their notation) (Ω, \mathcal{F}) being \mathbb{R}^d equipped with its Borel σ -algebra, $X = \mathcal{M}(\mathbb{R}^d)$ and Y equal to the space of bounded measurable functions on \mathbb{R}^d , we get that (X, Y) is ν -decomposable with $\Xi = \{\emptyset\}$, so that $\text{ess im}_\Xi(h) = \text{ran}(h)$, and thus

$$\sup_{\mu \in \mathcal{M}_+(\mathbb{R}^d)} \{ \langle h, \mu \rangle_{\mathcal{C}_0 \times \mathcal{M}} - D_{f,\nu}(\mu) \} = \begin{cases} \mathbb{E}_\nu[f^* \circ h], & \text{if } \text{ran}(h) \subset \overline{\text{dom}(f^*)}, \\ \infty, & \text{else.} \end{cases}$$

for any $h \in Y$, so in particular for any $h \in \mathcal{H}_K$. □

Next, we establish the link between $D_{f,\nu}^\lambda$ and the Moreau envelope of $G_{f,\nu}$.

Corollary 9. *For any fixed $\nu \in \mathcal{M}_+(\mathbb{R}^d)$ let $G_{f,\nu}$ be defined by (16). Then, it holds for $\mu \in \mathcal{M}(\mathbb{R}^d)$ that*

$$D_{f,\nu}^\lambda(\mu) = G_{f,\nu}^\lambda(m_\mu). \quad (20)$$

Proof. Since $G_{f,\nu} \in \Gamma_0(\mathcal{H}_K)$, we have that

$$G_{f,\nu}^\lambda(m_\mu) = \min_{g \in \mathcal{H}_K} \left\{ G_{f,\nu}(g) + \frac{1}{2\lambda} \|g - m_\mu\|_{\mathcal{H}_K}^2 \right\} \quad (21)$$

is well-defined and clearly the unique minimizer fulfills $g \in \text{ran}(m)$. Hence we can substitute $g = m_\sigma$ for $\sigma \in \mathcal{M}_+(\mathbb{R}^d)$ to obtain

$$G_{f,\nu}^\lambda(m_\mu) = \min_{\sigma \in \mathcal{M}_+(\mathbb{R}^d)} \left\{ D_{f,\nu}(\sigma) + \frac{1}{2\lambda} \|m_\mu - m_\sigma\|_{\mathcal{H}_K}^2 \right\},$$

which yields the assertion. \square

3.3 Properties of MMD-regularized f -Divergences

Now, we combine Corollary 9 with the properties of Moreau envelopes in Theorem 1 to prove various properties of the MMD-regularized functional $D_{f,\nu}^\lambda$ in a sequence of corollaries. For the KL divergence and the χ^2 -divergence, these properties have been shown differently in [27, 18] without using Moreau envelopes.

Corollary 10 (Dual formulation). *For $\nu \in \mathcal{M}_+(\mathbb{R}^d)$ and $\mu \in \mathcal{M}(\mathbb{R}^d)$, we have that*

$$D_{f,\nu}^\lambda(\mu) = \max_{\substack{p \in \mathcal{H}_K \\ p(\mathbb{R}^d) \subseteq \text{dom}(f^*)}} \left\{ \mathbb{E}_\mu[p] - \mathbb{E}_\nu[f^* \circ p] - \frac{\lambda}{2} \|p\|_{\mathcal{H}_K}^2 \right\}. \quad (22)$$

If $\hat{p} \in \mathcal{H}_K$ maximizes (22), then $\hat{g} = m_\mu - \lambda \hat{p}$ minimizes (21) and vice versa. Further, it holds

$$\frac{\lambda}{2} \|\hat{p}\|_{\mathcal{H}_K}^2 \leq D_{f,\nu}^\lambda(\mu) \leq \|\hat{p}\|_{\mathcal{H}_K} d_K(\mu, \nu), \quad (23)$$

and, in particular,

$$D_{f,\nu}^\lambda(\mu) \leq \|\hat{p}\|_{\mathcal{H}_K} (\|m_\mu\|_{\mathcal{H}_K} + \|m_\nu\|_{\mathcal{H}_K}) \quad \text{and} \quad \|\hat{p}\|_{\mathcal{H}_K} \leq \frac{2}{\lambda} d_K(\mu, \nu).$$

Proof. i) From Corollary 9 and Theorem 1(i)), we obtain

$$D_{f,\nu}^\lambda(\mu) = G_{f,\nu}^\lambda(m_\mu) = \max_{p \in \mathcal{H}_K} \left\{ \langle p, m_\mu \rangle_{\mathcal{H}_K} - G_{f,\nu}^*(p) - \frac{\lambda}{2} \|p\|_{\mathcal{H}_K}^2 \right\}.$$

By (4), we have $\langle p, m_\mu \rangle_{\mathcal{H}_K} = \mathbb{E}_\mu[p]$ and plugging this into (19) yields the first assertion. By Theorem 1 we also get the primal-dual relation.

ii) Using (20), there exists a $\hat{g} \in \text{dom}(G_{f,\nu})$ such that

$$D_{f,\nu}^\lambda(\mu) = G_{f,\nu}(\hat{g}) + \frac{1}{2\lambda} \|\hat{g} - m_\mu\|_{\mathcal{H}_K}^2 \geq \frac{1}{2\lambda} \|\hat{g} - m_\mu\|_{\mathcal{H}_K}^2 = \frac{\lambda}{2} \|\hat{p}\|_{\mathcal{H}_K}^2, \quad (24)$$

which is the first lower estimate. For the upper one, we use that $f(1) = 0$, so that $f^*(p) \geq p$ for all $p \in \mathbb{R}$. Then, together with (4), the upper estimate follows by

$$D_{f,\nu}^\lambda(\mu) = \mathbb{E}_\mu[\hat{p}] - \mathbb{E}_\nu[f^* \circ \hat{p}] - \frac{\lambda}{2} \|\hat{p}\|_{\mathcal{H}_K}^2 \leq \mathbb{E}_{\mu-\nu}[\hat{p}] \leq \|\hat{p}\|_{\mathcal{H}_K} \|m_\mu - m_\nu\|_{\mathcal{H}_K},$$

where we employed the Cauchy-Schwarz inequality in \mathcal{H}_K and (24). □

Remark 11. In [27, Eq. (2)], Glaser et al. introduced a so-called KALE functional. This is exactly the dual formulation (22) multiplied by $1 + \lambda$ for the Kullback-Leibler entropy function f_{KL} from Table 1. As expected, the dual function of the KALE functional [27, Eq. (6)] coincides with our primal formulation (14). Indeed, we have $D_f(\sigma | \nu) < \infty$ if and only if there exists a density $\rho \in L^1(\mathbb{R}^d, \nu; \mathbb{R}_{\geq 0})$ such that $\sigma = \rho\nu$. Thus,

$$\min_{\sigma \in \mathcal{M}_+(\mathbb{R}^d)} D_f(\sigma | \nu) + \frac{1}{2\lambda} d_K(\mu, \sigma)^2 = \min_{\substack{\rho \in L^1(\mathbb{R}^d) \\ \rho \geq 0}} \int_{\mathbb{R}^d} f_{\text{KL}} \circ \rho \, d\nu + \frac{1}{2\lambda} \|m_{\rho\nu} - m_\mu\|_{\mathcal{H}_K}^2.$$

We now discuss topological properties of $D_{f,\nu}^\lambda$, generalizing [27, Thm. 1], where only metrization of $\mathcal{P}_1(\mathbb{R}^d) \subset B_{\varphi(0)}(0)$ is shown.

Corollary 12 (Topological properties).

- i) For every $\nu \in \mathcal{M}_+(\mathbb{R}^d)$, the function $D_{f,\nu}^\lambda : \mathcal{M}(\mathbb{R}^d) \rightarrow \mathbb{R}$ is weakly continuous.
- ii) If D_f is a divergence, then D_f^λ in (14) is a divergence as well.
- iii) If D_f is a divergence, then D_f^λ “metrizes” the topology on the closed balls $B_r(\mu_0) := \{\mu \in \mathcal{M}_+(\mathbb{R}^d) : d_K(\mu, \mu_0) \leq r\} \subset (\mathcal{M}_+(\mathbb{R}^d), d_K)$ for any $r > 0$ and any $\mu_0 \in \mathcal{M}_+(\mathbb{R}^d)$ in the sense that for $\mu_n, \mu \in B_r(\mu_0)$ it is equivalent that $D_f^\lambda(\mu_n | \mu) \rightarrow 0$ and that $d_K(\mu_n, \mu) \rightarrow 0$.

Proof. i) Let $(\mu_n)_{n \in \mathbb{N}}$ converge weakly to μ , i.e., $\lim_{n \rightarrow \infty} \langle f, \mu_n \rangle = \langle f, \mu \rangle$ for all $f \in \mathcal{C}_b(\mathbb{R}^d)$. Then, we have by [73, Lemma 10] that $m_{\mu_n} \rightarrow m_\mu$ in \mathcal{H}_K . Since $G_{f,\nu}^\lambda$ is continuous by Theorem 1(iii)), this implies together with Corollary 9 that

$$D_{f,\nu}^\lambda(\mu) = G_{f,\nu}^\lambda(m_\mu) = \lim_{n \rightarrow \infty} G_{f,\nu}^\lambda(m_{\mu_n}) = \lim_{n \rightarrow \infty} D_{f,\nu}^\lambda(\mu_n).$$

- ii) The definiteness follows from (14) since both summands are non-negative. We refer to [12, Thm. 75.4] for a more detailed proof in a slightly different setting.
- iii) Since f has its unique minimizer at $x = 1$, we have $0 \in \partial f(x)$ only for $x = 1$. Hence, $\partial f^*(0) = \{1\}$, and thus f^* is differentiable at zero with $(f^*)'(0) = 1$. Let

$\mu_n, \mu \in B_r(\mu_0)$ for all $n \in \mathbb{N}$. As $G_{f,\nu}^\lambda$ is continuous, the relation $d_K(\mu_n, \mu) = \|m_{\mu_n} - m_\mu\|_{\mathcal{H}_K} \rightarrow 0$ implies $D_f^\lambda(\mu_n | \mu) = G_{f,\mu}^\lambda(m_{\mu_n}) \rightarrow D_f^\lambda(\mu | \mu) = 0$.

For the reverse direction, assume that $D_f^\lambda(\mu_n | \mu) \rightarrow 0$. For any $n \in \mathbb{N}$, we define $g_n := m_{\mu_n - \mu} = m_{\mu_n} - m_\mu$, for which it holds that

$$\|g_n\|_{\mathcal{C}_0} \leq C \|g_n\|_{\mathcal{H}_K} = C d_K(\mu_n, \mu) \leq C(d_K(\mu_n, \mu_0) + d_K(\mu_0, \mu)) \leq 2Cr, \quad (25)$$

where $C > 0$ is the embedding constant from $\mathcal{H}_K \hookrightarrow \mathcal{C}_0(\mathbb{R}^d)$. Hence, it holds for any $\frac{f'_\infty}{2Cr} > \epsilon > 0$ that $\epsilon g_n(\mathbb{R}^d) \subset \text{dom}(f^*)$ since $\epsilon |g_n(x)| < \frac{f'_\infty}{2Cr} |g_n(x)| \leq f'_\infty$ for all $x \in \mathbb{R}^d$. By (22), we further get that

$$\begin{aligned} D_f^\lambda(\mu_n | \mu) &\geq \mathbb{E}_{\mu_n}(\epsilon g_n) - \mathbb{E}_\mu(f^* \circ (\epsilon g_n)) - \frac{\lambda \epsilon^2}{2} \|g_n\|_{\mathcal{H}_K}^2 \\ &= \epsilon \|g_n\|_{\mathcal{H}_K}^2 - \mathbb{E}_\mu[f^* \circ (\epsilon g_n) - \epsilon g_n] - \frac{\lambda \epsilon^2}{2} \|g_n\|_{\mathcal{H}_K}^2 \\ &= \left(\epsilon - \frac{\lambda \epsilon^2}{2}\right) \|g_n\|_{\mathcal{H}_K}^2 - \mathbb{E}_\mu[f^* \circ (\epsilon g_n) - \epsilon g_n]. \end{aligned} \quad (26)$$

Using Taylor's theorem with the Peano form of the remainder, there exists $h: (-\infty, f'_\infty) \rightarrow \mathbb{R}$ with $\lim_{t \rightarrow 0} \frac{h(t)}{t} = 0$ such that $f^*(t) = t + h(t)$ for all $t \in (-\infty, f'_\infty)$. Thus, we get

$$\mathbb{E}_\mu[f^* \circ (\epsilon g_n) - \epsilon g_n] = \int_{\mathbb{R}^d} h \circ (\epsilon g_n) d\mu \leq \left\| \frac{h \circ (\epsilon g_n)}{\epsilon g_n} \right\|_\infty \|\epsilon g_n\|_\infty \mu(\mathbb{R}^d) \quad (27)$$

with the convention $\frac{h(\epsilon g_n(x))}{\epsilon g_n(x)} = 0$ if $g_n(x) = 0$. Plugging (27) into (26) yields

$$D_f^\lambda(\mu_n | \mu) \geq \epsilon \|g_n\|_{\mathcal{H}_K} \left(\left(1 - \frac{\lambda}{2}\epsilon\right) \|g_n\|_{\mathcal{H}_K} - C \left\| \frac{h \circ (\epsilon g_n)}{\epsilon g_n} \right\|_\infty \mu(\mathbb{R}^d) \right). \quad (28)$$

Since $\lim_{t \rightarrow 0} \frac{h(t)}{t} = 0$ and ϵg_n is uniformly bounded, equation (25) implies that the second factor in (28) converges to $\|g_n\|_{\mathcal{H}_K}$ for $\epsilon \searrow 0$. Thus, we can pick $\epsilon > 0$ independent of n such that $D_f^\lambda(\mu_n | \mu) \geq \frac{\epsilon}{2} \|g_n\|_{\mathcal{H}_K}^2 = \frac{\epsilon}{2} d_K(\mu_n, \mu)^2$. From this, we infer $d_K(\mu_n, \mu) \rightarrow 0$. □

Now, we investigate the two asymptotic regimes of D_f^λ .

Corollary 13 (Limits for $\lambda \rightarrow 0$ and $\lambda \rightarrow \infty$).

i) It holds $\lim_{\lambda \rightarrow 0} D_{f,\nu}^\lambda(\mu) = D_{f,\nu}(\mu)$ for $\mu, \nu \in \mathcal{M}_+(\mathbb{R}^d)$.

ii) We have that $D_{f,\nu}^\lambda$ converges to $D_{f,\nu}$ in the sense of Mosco: For $\mu \in \mathcal{M}_+(\mathbb{R}^d)$, a monotonically decreasing $(\lambda_n)_{n \in \mathbb{N}} \subset (0, \infty)$ with $\lambda_n \rightarrow 0$, and $(\mu_n)_{n \in \mathbb{N}} \subset \mathcal{M}_+(\mathbb{R}^d)$ with $\mu_n \rightarrow \mu$ it holds that

$$D_{f,\nu}(\mu) \leq \liminf_{n \rightarrow \infty} D_{f,\nu}^{\lambda_n}(\mu_n).$$

Further, there exists a sequence $(\tilde{\mu}_n)_{n \in \mathbb{N}} \subset \mathcal{M}_+(\mathbb{R}^d)$ with $\mu_n \rightarrow \mu$ such that

$$D_{f,\nu}(\mu) = \lim_{n \rightarrow \infty} D_{f,\nu}^{\lambda_n}(\tilde{\mu}_n).$$

iii) For any $r > 0$ and any $\mu_0 \in \mathcal{M}_+(\mathbb{R}^d)$, it holds

$$\lim_{\lambda \rightarrow \infty} \sup_{\mu \in B_r(\mu_0)} \left| (1 + \lambda) D_f^\lambda(\mu | \nu) - \frac{1}{2} d_K(\mu, \nu)^2 \right| = 0.$$

Proof.

- i) Since $f'_\infty > 0$, we have $0 \in \text{int}(\text{dom}(f^*))$. By Theorem 1(iii), we get pointwise convergence to $G_{\nu,f}$. Then, the statement follows by the final part of Lemma 8 and Corollary 9.
- ii) By Theorem 1(iii), the sequences $(G_{f,\nu}^{\lambda_n}(h))_{n \in \mathbb{N}}$ are monotonically increasing with $\sup_{n \in \mathbb{N}} G_{f,\nu}^{\lambda_n}(h) = G_{f,\nu}(h)$ for any $h \in \mathcal{H}_K$. As $G_{f,\nu}$ is lower semicontinuous, [17, Rem. 2.12] implies that $(G_{f,\nu}^{\lambda_n})_{n \in \mathbb{N}}$ Γ -converges to $G_{\nu,f}$. More precisely, it holds that $G_{f,\nu}(h) \leq \liminf_{n \rightarrow \infty} G_{f,\nu}^{\lambda_n}(h_n)$ for every $h \in \mathcal{H}_K$ and any sequence $(h_n)_{n \in \mathbb{N}} \subset \mathcal{H}_K$ with $h_k \rightarrow h$. Further, for every $h \in \mathcal{H}_K$ it holds that $G_{f,\nu}(h) = \lim_{n \rightarrow \infty} G_{f,\nu}^{\lambda_n}(h)$. The statement now follows from the fact that $D_{f,\nu}^\lambda = G_{\nu,f}^\lambda \circ m$ by Corollary 9 and since $\mu_n \rightarrow \mu$ in $\mathcal{M}_+(\mathbb{R}^d)$ implies $m_{\mu_n} \rightarrow m_\mu$ by [73, Lemma 10].
- iii) From (14), we infer $(1 + \lambda) D_f^\lambda(\mu | \nu) \leq \frac{1+\lambda}{2\lambda} d_K(\mu, \nu)^2$. To get a lower bound, we proceed as for Corollary 12(iii). For $g_{\mu,\lambda} := \frac{1}{\lambda} m_{\mu-\nu}$ with $\lambda > \frac{C}{f'_\infty} |\mu - \nu|(\mathbb{R}^d) > 0$, we have that $g_{\mu,\lambda}(\mathbb{R}^d) \subset \text{dom}(f^*)$. Analogously to (26) and (28) (using the same h), we get

$$\begin{aligned} (1 + \lambda) D_f^\lambda(\mu | \nu) &\geq \frac{(1 + \lambda)}{\lambda} d_K(\mu, \nu) \left(\frac{1}{2} d_K(\mu, \nu) - C\nu(\mathbb{R}^d) \left\| \frac{h \circ g_{\mu,\lambda}}{g_{\mu,\lambda}} \right\|_\infty \right) \\ &\geq \frac{1}{2} d_K(\mu, \nu)^2 - C\nu(\mathbb{R}^d) d_K(\mu, \nu) \frac{1 + \lambda}{\lambda} \left\| \frac{h \circ g_{\mu,\lambda}}{g_{\mu,\lambda}} \right\|_\infty. \end{aligned} \quad (29)$$

Combining (29) with $(1 + \lambda)D_f^\lambda(\mu | \nu) \leq \frac{1+\lambda}{2\lambda}d_K(\mu, \nu)^2$, we get for $\mu \in B_r(\mu_0)$ that

$$\begin{aligned} & \left| (1 + \lambda)D_{f,\nu}^\lambda(\mu) - \frac{1}{2}d_K(\mu, \nu)^2 \right| \\ & \leq d_K(\mu, \nu) \max \left(\frac{d_K(\mu, \nu)}{2\lambda}, C\nu(\mathbb{R}^d) \frac{1 + \lambda}{\lambda} \left\| \frac{h \circ g_{\mu,\lambda}}{g_{\mu,\lambda}} \right\|_\infty \right) \\ & \leq (d_K(\mu_0, \nu) + r) \max \left(\frac{d_K(\mu_0, \nu) + r}{2\lambda}, C\nu(\mathbb{R}^d) \frac{1 + \lambda}{\lambda} \left\| \frac{h \circ g_{\mu,\lambda}}{g_{\mu,\lambda}} \right\|_\infty \right). \end{aligned}$$

Here, the first term in the maximum converges to zero as $\lambda \rightarrow \infty$. As for Corollary 12(iii), $\|g_{\mu,\lambda}\|_\infty \leq \frac{C}{\lambda}(d_K(\mu_0, \nu) + r)$ together with $\lim_{t \rightarrow 0} \frac{1}{t}h(t) = 0$ yields that also the second term converges to zero. Thus, the claim follows. \square

The Moreau envelope interpretation of $D_{f,\nu}^\lambda$ allows the calculation of its gradient without the implicit function theorem, which is used to justify the calculations for the KALE functional in [27, Lem. 2]. Furthermore, we strengthen their result by proving Fréchet differentiability instead of Gâteaux differentiability.

Corollary 14 (Gradient). *The function $D_{f,\nu}^\lambda: \mathcal{M}(\mathbb{R}^d) \rightarrow [0, \infty)$ is Fréchet differentiable and $\nabla D_{f,\nu}^\lambda(\mu) = \hat{p}$, where $\hat{p} \in \mathcal{H}_K$ is the maximizer in (22). Further, the mapping $\nabla D_{f,\nu}^\lambda: \mathcal{M}(\mathbb{R}^d) \rightarrow \mathcal{C}_0(\mathbb{R}^d)$ is $\frac{1}{\lambda}$ -Lipschitz with respect to d_K .*

Proof. By Theorem 1(ii) and Corollary 10, we obtain

$$\nabla G_{f,\nu}^\lambda(m_\mu) = \lambda^{-1}(m_\mu - \text{prox}_{\lambda G_{f,\nu}}(m_\mu)) = \hat{p}.$$

As a concatenation of a Fréchet differentiable and a continuous linear mapping, $D_{f,\nu}^\lambda = G_{f,\nu}^\lambda \circ m$ is Fréchet differentiable. The Fréchet derivative of the KME $m: \mathcal{M}(\mathbb{R}^d) \rightarrow \mathcal{H}_K$ at $\mu \in \mathcal{M}(\mathbb{R}^d)$ is $dm_\mu = m \in L(\mathcal{M}(\mathbb{R}^d); \mathcal{H}_K)$. Using these computations together with the chain rule, we get for any $\sigma \in \mathcal{M}(\mathbb{R}^d)$ that

$$dD_{f,\nu}^\lambda(\mu)[\sigma] = d(G_{f,\nu}^\lambda \circ m)(\mu)[\sigma] = dG_{f,\nu}^\lambda(m_\mu)[m_\sigma] = \langle \hat{p}, \sigma \rangle_{\mathcal{C}_0 \times \mathcal{M}}.$$

Hence, we identify $\nabla D_{f,\nu}^\lambda(\mu) = \hat{p} \in \mathcal{C}_0(\mathbb{R}^d)$. Finally, we have by Theorem 1(ii) that

$$\|\nabla G_{f,\nu}^\lambda(m_\mu) - \nabla G_{f,\nu}^\lambda(m_\sigma)\|_{\mathcal{C}_0} \leq \lambda^{-1}\|m_\mu - m_\sigma\|_{\mathcal{H}_K} = \lambda^{-1}d_K(\mu, \sigma),$$

which completes the proof. \square

4 Wasserstein Gradient Flows of Regularized f -Divergences

Now, we discuss Wasserstein gradient flows of $D_{f,\nu}^\lambda$. This requires some preliminaries from [4, Secs. 8.3, 9.2, 11.2], which we adapt to our setting in Section 4.1.

4.1 Wasserstein Gradient Flows

We consider the *Wasserstein space* $\mathcal{P}_2(\mathbb{R}^d)$ of Borel probability measures with finite second moments, equipped with the *Wasserstein distance*

$$W_2(\mu, \nu)^2 := \min_{\pi \in \Gamma(\mu, \nu)} \int_{\mathbb{R}^d \times \mathbb{R}^d} \|x - y\|_2^2 d\pi(x, y), \quad (30)$$

where $\Gamma(\mu, \nu) = \{\pi \in \mathcal{P}_2(\mathbb{R}^d \times \mathbb{R}^d) : (P_1)_\# \pi = \mu, (P_2)_\# \pi = \nu\}$. Here, $T_\# \mu := \mu \circ T^{-1}$ denotes the *push-forward* of μ via the measurable map T , and $P_i(x) := x_i$, $i = 1, 2$, for $x = (x_1, x_2) \in \mathbb{R}^d \times \mathbb{R}^d$.

A curve $\gamma: [0, 1] \rightarrow \mathcal{P}_2(\mathbb{R}^d)$, $t \mapsto \gamma_t$ is a *geodesic* if $W_2(\gamma_s, \gamma_t) = W_2(\gamma_0, \gamma_1)|t - s|$ for all $s, t \in [0, 1]$. The Wasserstein space is geodesic, i.e., any measures $\mu_0, \mu_1 \in \mathcal{P}_2(\mathbb{R}^d)$ can be connected by a geodesic. These are all of the form

$$\gamma_t = ((1 - t)P_1 + tP_2)_\# \hat{\pi}, \quad t \in [0, 1],$$

where $\hat{\pi} \in \Gamma(\mu_0, \mu_1)$ realizes $W_2(\mu_0, \mu_1)$ in (30).

For $\mathcal{F}: \mathcal{P}_2(\mathbb{R}^d) \rightarrow (-\infty, \infty]$, we set $\text{dom}(\mathcal{F}) := \{\mu \in \mathcal{P}_2(\mathbb{R}^d) : \mathcal{F}(\mu) < \infty\}$. The function \mathcal{F} is *M-convex along geodesics* with $M \in \mathbb{R}$ if, for every $\mu_0, \mu_1 \in \text{dom}(\mathcal{F})$, there exists a geodesic $\gamma: [0, 1] \rightarrow \mathcal{P}_2(\mathbb{R}^d)$ between μ_0 and μ_1 such that

$$\mathcal{F}(\gamma_t) \leq (1 - t)\mathcal{F}(\mu_0) + t\mathcal{F}(\mu_1) - \frac{M}{2} t(1 - t) W_2(\mu_0, \mu_1)^2, \quad t \in [0, 1].$$

Frequently, we need a more general notion of convexity. Based on the set of three-plans with base $\sigma \in \mathcal{P}_2(\mathbb{R}^d)$ given by

$$\Gamma_\sigma(\mu, \nu) := \{\alpha \in \mathcal{P}_2(\mathbb{R}^d \times \mathbb{R}^d \times \mathbb{R}^d) : (P_1)_\# \alpha = \sigma, (P_2)_\# \alpha = \mu, (P_3)_\# \alpha = \nu\},$$

a *generalized geodesic* $\gamma_\alpha: [0, 1] \rightarrow \mathcal{P}_2(\mathbb{R}^d)$ joining μ and ν with base σ is defined as

$$\gamma_{\alpha,t} := ((1 - t)P_2 + tP_3)_\# \alpha, \quad t \in [0, 1],$$

where $\alpha \in \Gamma_\sigma(\mu, \nu)$ with $(P_{1,2})_\# \alpha \in \Gamma^{\text{opt}}(\sigma, \mu)$ and $(P_{1,3})_\# \alpha \in \Gamma^{\text{opt}}(\sigma, \nu)$. Here, $\Gamma^{\text{opt}}(\mu, \nu)$ denotes the *set of optimal transport plans* that minimize (30). The plan α can be interpreted as transport from μ to ν via σ . A function $\mathcal{F}: \mathcal{P}_2(\mathbb{R}^d) \rightarrow (-\infty, \infty]$ is *M-convex along generalized geodesics* if, for every $\sigma, \mu, \nu \in \text{dom}(\mathcal{F})$, there exists a generalized geodesic $\gamma_\alpha: [0, 1] \rightarrow \mathcal{P}_2(\mathbb{R}^d)$ such that

$$\mathcal{F}(\gamma_{\alpha,t}) \leq (1 - t)\mathcal{F}(\mu) + t\mathcal{F}(\nu) - \frac{M}{2} t(1 - t) W_\alpha^2(\mu, \nu), \quad t \in [0, 1],$$

where

$$W_\alpha^2(\mu, \nu) := \int_{\mathbb{R}^d \times \mathbb{R}^d \times \mathbb{R}^d} \|y - z\|_2^2 d\alpha(x, y, z).$$

Each function that is M -convex along generalized geodesics is also M -convex along geodesics since generalized geodesics with base $\sigma = \mu$ are actual geodesics.

The *strong (reduced) Fréchet subdifferential* $\partial\mathcal{F}(\mu)$ of a proper, lower semicontinuous, geodesically convex function $\mathcal{F}: \mathcal{P}_2(\mathbb{R}^d) \rightarrow (-\infty, \infty]$ at μ consists of $v \in L_2(\mathbb{R}^d, \mu; \mathbb{R}^d)$ such that for every $\eta \in \mathcal{P}_2(\mathbb{R}^d)$ and every $\pi \in \Gamma(\mu, \eta)$, it holds

$$\mathcal{F}(\eta) - \mathcal{F}(\mu) \geq \int_{\mathbb{R}^d \times \mathbb{R}^d} \langle v(x_1), x_2 - x_1 \rangle d\pi(x_1, x_2) + o(C_2(\pi)), \quad (31)$$

where $C_2(\pi)^2 := \int_{\mathbb{R}^d \times \mathbb{R}^d} \|x_1 - x_2\|_2^2 d\pi(x_1, x_2)$ and the asymptotic $o(\cdot)$ has to be understood with respect to the W_2 metric, see [4, Eq. (10.3.7)].

A curve $\gamma: (0, \infty) \rightarrow \mathcal{P}_2(\mathbb{R}^d)$ is called *locally 2-absolutely continuous* if there exists a Borel velocity field $v: \mathbb{R}^d \times (0, \infty) \rightarrow \mathbb{R}^d$, $(x, t) \mapsto v_t(x)$ with $(t \mapsto \|v_t\|_{L^2(\mathbb{R}^d; \gamma_t)}) \in L_{\text{loc}}^2(0, \infty)$ such that the continuity equation

$$\partial_t \gamma_t + \nabla \cdot (v_t \gamma_t) = 0$$

is fulfilled on $(0, \infty) \times \mathbb{R}^d$ in a weak sense, i.e.,

$$\int_0^\infty \int_{\mathbb{R}^d} \partial_t \varphi(t, x) + \langle \nabla_x \varphi(t, x), v_t(x) \rangle d\gamma_t(x) dt = 0 \quad \text{for all } \varphi \in \mathcal{C}_c^\infty((0, \infty) \times \mathbb{R}^d).$$

A locally 2-absolutely continuous curve $\gamma: (0, \infty) \rightarrow \mathcal{P}_2(\mathbb{R}^d)$ with velocity field v_t in the regular tangent space

$$\mathbb{T}_{\gamma_t} \mathcal{P}_2(\mathbb{R}^d) := \overline{\{\nabla \phi : \phi \in \mathcal{C}_c^\infty(\mathbb{R}^d)\}}^{L_2(\mathbb{R}^d, \gamma_t; \mathbb{R}^d)}$$

of $\mathcal{P}_2(\mathbb{R}^d)$ at γ_t is called a *Wasserstein gradient flow of $\mathcal{F}: \mathcal{P}_2(\mathbb{R}^d) \rightarrow (-\infty, \infty]$* if

$$v_t \in -\partial\mathcal{F}(\gamma_t), \quad \text{for a.e. } t > 0. \quad (32)$$

In principle, (32) involves the so-called reduced Fréchet subdifferential $\partial\mathcal{F}$. We will show the $D_{f, \nu}^\lambda$ are Fréchet differentiable such that we can use the strong Fréchet subdifferential in (31) instead. Then, we have the following theorem [4, Thm. 11.2.1].

Theorem 15. *Assume that $\mathcal{F}: \mathcal{P}_2(\mathbb{R}^d) \rightarrow (-\infty, \infty]$ is proper, lower semicontinuous, coercive and M -convex along generalized geodesics. Given $\mu_0 \in \overline{\text{dom}(\mathcal{F})}$, there exists a unique Wasserstein gradient flow of \mathcal{F} with $\gamma(0+) = \mu_0$.*

Remark 16. *By [4, Eq. (11.2.1b)] any proper M -convex functional that is bounded from below by some constant is coercive in the sense of [4, Eq. (2.1.2b)].*

4.2 Wasserstein Gradient Flow of $D_{f,\nu}^\lambda$

Now, we show that $D_{f,\nu}^\lambda$ is locally Lipschitz, M -convex along generalized geodesics, and that $\partial D_{f,\nu}^\lambda(\mu)$ is a singleton for every $\mu \in \mathcal{P}_2(\mathbb{R}^d)$. To this end, we rely on [83, Prop. 2, Cor. 3], which we adapt to our setting in the following lemma.

Lemma 17. *Let the kernel K fulfill $K(x, x) + K(y, y) - 2K(x, y) \leq C_{\text{emb}}^2 \|x - y\|_2^2$ with some constant $C_{\text{emb}} > 0$. Then, it holds*

$$d_K(\mu, \nu) \leq C_{\text{emb}} W_2(\mu, \nu). \quad (33)$$

If $K(x, y) = \Phi(x - y)$ is translation invariant, then we get $C_{\text{emb}} = \sqrt{\lambda_{\max}(-\nabla^2 \Phi(0))}$. For radial kernels $K(x, y) = \phi(\|x - y\|_2^2)$, we have

$$\nabla^2 \Phi(x) = 4\phi''(\|x\|_2^2)xx^\top + 2\phi'(\|x\|_2^2) \text{id},$$

so that $C_{\text{emb}} = \sqrt{-2\phi'(0)}$.

Note that the authors in [83] found $C_{\text{emb}} = \sqrt{\lambda_{\max}(-\nabla^2 \Phi(0))} \Phi(0)$ instead, which we could not verify. Now, we prove the local Lipschitz continuity of $D_{f,\nu}^\lambda$ with Theorem 1(ii) and Lemma 17.

Lemma 18. *The function $D_{f,\nu}^\lambda: (\mathcal{P}_2(\mathbb{R}^d), W_2) \rightarrow [0, \infty)$ is locally Lipschitz continuous.*

Proof. By Theorem 1(ii), we know that $G_{f,\nu}^\lambda: \mathcal{H}_K \rightarrow [0, \infty)$ is continuously Fréchet differentiable. Hence, it is locally Lipschitz continuous. Since $m: (\mathcal{P}_2(\mathbb{R}^d), d_K) \rightarrow \mathcal{H}_K$ is an isometry and $G_{f,\nu}^\lambda \circ m$, the claim follows using (33). \square

Next, we show the M -convexity of $D_{f,\nu}^\lambda$ along generalized geodesics. Our Moreau envelope interpretation simplifies the proof in [27, Lem. 4] since we do not need to invoke the implicit function theorem.

Theorem 19. *Let $K(x, y) = \phi(\|x - y\|_2^2)$ with $\phi \in \mathcal{C}^2([0, \infty))$. Then, $D_{f,\nu}^\lambda: \mathcal{P}_2(\mathbb{R}^d) \rightarrow [0, \infty)$ is $(-M)$ -convex along generalized geodesics with $M := \frac{8}{\lambda} \sqrt{(d+2)\phi''(0)\phi(0)}$.*

Proof. Let $\mu_1, \mu_2, \mu_3 \in \mathcal{P}_2(\mathbb{R}^d)$ and $\gamma: [0, 1] \rightarrow \mathcal{P}_2(\mathbb{R}^d)$, $t \mapsto ((1-t)P_2 + tP_3)_\# \alpha$ be a generalized geodesic associated to a three-plan $\alpha \in \Gamma_{\mu_1}(\mu_2, \mu_3)$. Furthermore, $\tilde{\gamma}: [0, 1] \rightarrow \mathcal{P}_2(\mathbb{R}^d)$, $t \mapsto (1-t)\mu_2 + t\mu_3$ denotes the linear interpolation between μ_2 and μ_3 . Since $G_{f,\nu}^\lambda$ and $D_{f,\nu}^\lambda$ are linearly convex, it holds for $t \in [0, 1]$ that

$$\begin{aligned} D_{f,\nu}^\lambda(\gamma_t) &\leq (1-t)D_{f,\nu}^\lambda(\mu_2) + tD_{f,\nu}^\lambda(\mu_3) + D_{f,\nu}^\lambda(\gamma_t) - D_{f,\nu}^\lambda(\tilde{\gamma}_t) \\ &\leq (1-t)D_{f,\nu}^\lambda(\mu_2) + tD_{f,\nu}^\lambda(\mu_3) + \langle \nabla G_{f,\nu}^\lambda(m_{\gamma_t}), m_{\gamma_t} - m_{\tilde{\gamma}_t} \rangle_{\mathcal{H}_K}. \end{aligned}$$

We consider the third summand. Let \hat{p}_t maximize the dual formulation (2) of $G_{f,\nu}^\lambda(m_{\gamma_t})$. Then, we know by Theorem 1(ii) that $\nabla G_{f,\nu}^\lambda(m_{\gamma_t}) = \hat{p}_t$, so that

$$\begin{aligned} & \langle \nabla G_{f,\nu}^\lambda(m_{\gamma_t}), m_{\gamma_t} - m_{\tilde{\gamma}_t} \rangle_{\mathcal{H}_K} \\ &= \int_{\mathbb{R}^d \times \mathbb{R}^d \times \mathbb{R}^d} \hat{p}_t((1-t)y_2 + ty_3) - ((1-t)\hat{p}_t(y_2) + t\hat{p}_t(y_3)) \, d\alpha(y_1, y_2, y_3). \end{aligned}$$

Due to (7), $\nabla \hat{p}_t$ is Lipschitz continuous with $\text{Lip}(\nabla \hat{p}_t) \leq 2\|\hat{p}_t\|_{\mathcal{H}_K} \sqrt{\phi''(0)(d+2)}$. Hence, the descent lemma [51, Lemma 1.2.3, Eq. (1.2.12)] implies that \hat{p}_t is $(-\text{Lip}(\nabla \hat{p}_t))$ -convex (in the sense of [4, Def. 2.4.1]) as a function on the metric space $(\mathbb{R}^d, \|\cdot\|_2)$ and

$$\begin{aligned} \langle \nabla G_{f,\nu}^\lambda(m_{\gamma_t}), m_{\gamma_t} - \tilde{\gamma}_t \rangle_{\mathcal{H}_K} &\leq \frac{t(1-t)}{2} \text{Lip}(\nabla \hat{p}_t) \int_{\mathbb{R}^d \times \mathbb{R}^d \times \mathbb{R}^d} \|y_2 - y_3\|_2^2 \, d\alpha(y_1, y_2, y_3) \\ &= \frac{1}{2} \text{Lip}(\nabla \hat{p}_t) t(1-t) W_\alpha^2(\mu_2, \mu_3). \end{aligned}$$

By (23), we have $\|\hat{p}_t\|_{\mathcal{H}_K} \leq \frac{2}{\lambda} (\|m_{\gamma_t}\|_{\mathcal{H}_K} + \|m_\nu\|_{\mathcal{H}_K})$. For any $\mu \in \mathcal{P}_2(\mathbb{R}^d)$, it holds

$$\|m_\mu\|_{\mathcal{H}_K}^2 = \int_{\mathbb{R}^d \times \mathbb{R}^d} K(x, y) \, d\mu(y) \, d\mu(x) = \int_{\mathbb{R}^d \times \mathbb{R}^d} \phi(\|x - y\|_2^2) \, d\mu(y) \, d\mu(x) \leq \phi(0),$$

which implies

$$\|\hat{p}_t\|_{\mathcal{H}_K} \leq \frac{4}{\lambda} \sqrt{\phi(0)}. \quad (34)$$

Thus, for all $t \in [0, 1]$, we have $\text{Lip}(\nabla \hat{p}_t) \leq M := \frac{8}{\lambda} \sqrt{\phi(0)\phi''(0)(d+2)}$, and $D_{f,\nu}^\lambda$ is $-M$ -convex along generalized geodesics. \square

The next proposition determines the strong subdifferential of $D_{f,\nu}^\lambda$. The result generalizes [27, Lemma 3] to arbitrary f -divergences satisfying Assumption 3.

Lemma 20. *Let $K(x, y) = \phi(\|x - y\|_2^2)$ and $\phi \in \mathcal{C}^2([0, \infty))$. Then, it holds for any $\mu \in \mathcal{P}_2(\mathbb{R}^d)$ that $\partial D_{f,\nu}^\lambda(\mu) = \{\nabla \hat{p}\}$, where $\hat{p} \in \mathcal{H}_K$ maximizes (22).*

Proof. First, we show that $\nabla \hat{p} \in \partial D_{f,\nu}^\lambda(\mu)$. By convexity of $G_{f,\nu}^\lambda$ and Lemma 14, we obtain for any $\eta \in \mathcal{P}_2(\mathbb{R}^d)$ and any $\pi \in \Gamma(\mu, \eta)$ that

$$\begin{aligned} D_{f,\nu}^\lambda(\eta) - D_{f,\nu}^\lambda(\mu) &= G_{f,\nu}^\lambda(m_\eta) - G_{f,\nu}^\lambda(m_\mu) \geq \langle \nabla G_{f,\nu}^\lambda(m_\mu), m_\eta - m_\mu \rangle_{\mathcal{H}_K} \\ &= \langle \hat{p}, m_\eta - m_\mu \rangle_{\mathcal{H}_K} = \int_{\mathbb{R}^d} \hat{p}(x_2) \, d\eta(x_2) - \int_{\mathbb{R}^d} \hat{p}(x_1) \, d\mu(x_1) \\ &= \int_{\mathbb{R}^d \times \mathbb{R}^d} \hat{p}(x_2) - \hat{p}(x_1) \, d\pi(x_1, x_2). \end{aligned}$$

Combining (7) and (34), we get that $\hat{p} \in \mathcal{H}_K$ has a Lipschitz continuous gradient with Lipschitz constant $L := \frac{8}{\lambda} \sqrt{\phi(0)\phi''(0)(d+2)}$. Hence, we obtain by the descent lemma [51, Lemma 1.2.3] that

$$\begin{aligned} D_{f,\nu}^\lambda(\eta) - D_{f,\nu}^\lambda(\mu) &\geq \int_{\mathbb{R}^d \times \mathbb{R}^d} \langle \nabla \hat{p}(x_1), x_2 - x_1 \rangle - \frac{L}{2} \|x_2 - x_1\|_2^2 \, d\pi(x_1, x_2) \\ &= \int_{\mathbb{R}^d \times \mathbb{R}^d} \langle \nabla \hat{p}(x_1), x_2 - x_1 \rangle \, d\pi(x_1, x_2) - \frac{L}{2} C_2^2(\pi). \end{aligned} \quad (35)$$

Next, we show that $\nabla \hat{p}$ is the only subgradient. Suppose that $v: \mathbb{R}^d \rightarrow \mathbb{R}^d$ with $\|\cdot\|_2 \circ v \in L^2(\mathbb{R}^d, \mu)$ is in another subgradient. We define the perturbation map $A_t(x) := x - t(\nabla \hat{p}(x) - v(x))$ with $t > 0$, the perturbed measures $\mu_t := (A_t)_\# \mu$, and the induced plan $\pi_t := (\text{id}, A_t)_\# \mu \in \Gamma(\mu, \mu_t)$. For π_t it holds

$$C_2(\pi_t)^2 = \int_{\mathbb{R}^d} \|x - A_t(x)\|_2^2 \, d\mu(x) = t^2 \int_{\mathbb{R}^d} \|\nabla \hat{p}(x) - v(x)\|_2^2 \, d\mu(x) = t^2 C_2(\pi_1)^2. \quad (36)$$

Hence, $t \searrow 0$ implies $C_2(\pi_t) \rightarrow 0$. Since $G_{f,\nu}^\lambda$ is Fréchet differentiable, $T(\eta, \mu) := D_{f,\nu}^\lambda(\eta) - D_{f,\nu}^\lambda(\mu) - \langle \nabla G_{f,\nu}^\lambda(m_\mu), m_\eta - m_\mu \rangle_{\mathcal{H}_K}$ satisfies

$$\lim_{\|m_\eta - \mu\|_{\mathcal{H}_K} \rightarrow 0} \frac{T(\eta, \mu)}{\|m_\eta - \mu\|_{\mathcal{H}_K}} = 0.$$

Using a similar reasoning as for (35), we get

$$\begin{aligned} &D_{f,\nu}^\lambda(\mu_t) - D_{f,\nu}^\lambda(\mu) - \int_{\mathbb{R}^d \times \mathbb{R}^d} \langle v(x_1), x_2 - x_1 \rangle \, d\pi_t(x_1, x_2) \\ &= D_{f,\nu}^\lambda(\mu_t) - D_{f,\nu}^\lambda(\mu) - \int_{\mathbb{R}^d \times \mathbb{R}^d} \langle \nabla \hat{p}(x_1) - (\nabla \hat{p}(x_1) - v(x_1)), x_2 - x_1 \rangle \, d\pi_t(x_1, x_2) \\ &\leq T(\mu_t, \mu) + \frac{1}{2} LC_2(\pi_t)^2 + \int_{\mathbb{R}^d \times \mathbb{R}^d} \langle \nabla \hat{p}(x_1) - v(x_1), x_2 - x_1 \rangle \, d\pi_t(x_1, x_2) \\ &= T(\mu_t, \mu) + \frac{1}{2} LC_2(\pi_t)^2 - t \int_{\mathbb{R}^d \times \mathbb{R}^d} \|\nabla \hat{p}(x) - v(x)\|_2^2 \, d\mu(x) \\ &= T(\mu_t, \mu) + \frac{1}{2} LC_2(\pi_t)^2 - t C_2(\pi_1)^2. \end{aligned} \quad (37)$$

By (33) we have

$$d_K(\mu_t, \mu) \leq C_{\text{emb}} W_2(\mu_t, \mu) \leq C_{\text{emb}} C_2(\pi_t). \quad (38)$$

Using (36) and (38), we further estimate (37) as

$$\begin{aligned}
& \frac{1}{C_2(\pi_t)} \left(D_{f,\nu}^\lambda(\mu_t) - D_{f,\nu}^\lambda(\mu) - \int_{\mathbb{R}^d \times \mathbb{R}^d} \langle v(x_1), x_2 - x_1 \rangle d\pi_t(x_1, x_2) \right) \\
& \leq \frac{T(\mu_t, \mu) + \frac{1}{2}LC_2(\pi_t)^2 - tC_2(\pi_1)^2}{C_2(\pi_t)} \\
& \leq \frac{T(\mu_t, \mu)}{d_K(\mu_t, \mu)} \cdot C_{\text{emb}} + \frac{1}{2}LC_2(\pi_t) - C_2(\pi_1) \xrightarrow{t \searrow 0} -C_2(\pi_1).
\end{aligned}$$

Since $v \in \partial D_{f,\nu}^\lambda(\mu)$, we must have $C_2(\pi_1) = 0$. Hence, $\pi_1 \in \Gamma(\mu, \mu_1)$ implies that $\mu_1 = \mu$. Due to $\mu_1 = (A_1)_{\#}\mu$, we must have $\nabla \hat{p} = v$ μ -a.e. \square

Based on Theorem 15 and Lemma 20, we have the following result.

Corollary 21. *Let $K(x, y) = \phi(\|x - y\|_2^2)$ be a radial kernel and $\phi \in \mathcal{C}^2([0, \infty))$. For any $\gamma_t \in \mathcal{P}_2(\mathbb{R}^d)$, let \hat{p}_{γ_t} denote the maximizer in the dual formulation (22) of $D_{f,\nu}^\lambda(\gamma_t)$. Then, for any $\mu_0 \in \mathcal{P}_2(\mathbb{R}^d)$, the equation*

$$\partial_t \gamma_t - \text{div}(\gamma_t \nabla \hat{p}_{\gamma_t}) = 0. \quad (39)$$

has a unique weak solution γ_t fulfilling $\gamma(0+) = \mu_0$, where $\gamma(0+) := \lim_{t \searrow 0} \gamma_t$.

Wasserstein Gradient Flows for Empirical Measures. Finally, we investigate the Wasserstein gradient flow (39) starting in an empirical measure

$$\mu_0 := \frac{1}{N} \sum_{i=1}^N \delta_{x_i^{(0)}}. \quad (40)$$

To solve (39) numerically, we consider a *particle functional* $D_N: \mathbb{R}^{dN} \rightarrow [0, \infty)$ of $D_{f,\nu}^\lambda$ defined for $x := (x_1, \dots, x_N)$ as

$$D_N(x) := D_{\nu,f}^\lambda \left(\frac{1}{N} \sum_{k=1}^N \delta_{x_k} \right),$$

and consider the particle flow $x: [0, \infty) \rightarrow \mathbb{R}^{dN}$ with

$$\dot{x}(t) = -N \nabla D_N(x(t)), \quad x(0) := (x_1(0), \dots, x_N(0)). \quad (41)$$

In general, solutions of (41) differ from those of (39). However, for our setting, we can show that the flow (41) induces a Wasserstein gradient flow.

Proposition 22. *Assume that $K(x, y) = \phi(\|x - y\|_2^2)$ and $\phi \in \mathcal{C}^2([0, \infty))$. Let $x(t) = (x_i(t))_{i=1}^N \subset \mathbb{R}^{dN}$, $t \in [0, \infty)$, be a solution of (41). Then, the corresponding curve of empirical measures $\gamma_N: [0, \infty) \rightarrow \mathcal{P}_2(\mathbb{R}^d)$ given by*

$$\gamma_N(t) = \frac{1}{N} \sum_{i=1}^N \delta_{x_i(t)}$$

is a Wasserstein gradient flow of $D_{\nu, f}^\lambda$ starting in μ_0 .

Proof. For the vector-valued measure $M_N(t) := \frac{1}{N} \sum_{i=1}^N \dot{x}_i(t) \delta_{x_i(t)} = - \sum_{i=1}^N \nabla_{x_i} D_N(x) \delta_{x_i(t)}$ and $\varphi \in C_c^\infty((0, \infty) \times \mathbb{R}^d)$ it holds that

$$\begin{aligned} & \int_0^\infty \left(\int_{\mathbb{R}^d} \partial_t \varphi(t, x) d\gamma_N(t) + \int_{\mathbb{R}^d} \nabla_x \varphi(t, x) dM_N(t) \right) dt \\ &= \frac{1}{N} \sum_{i=1}^N \int_0^\infty (\partial_t \varphi(t, x_i(t)) + \nabla_x \varphi(t, x_i(t)) \cdot \dot{x}_i(t)) dt \\ &= \frac{1}{N} \sum_{i=1}^N \int_0^\infty \frac{d}{dt} \varphi(t, x_i(t)) dt = 0. \end{aligned}$$

Hence, $\partial_t \gamma_N + \operatorname{div}(M_N) = 0$ holds in weak sense. To show $M_N(t) = -\nabla \hat{p}_{\gamma_N(t)} \gamma_N(t)$, we first note that $D_N(x) = G_{f, \nu}^\lambda(m_{\gamma_N})$ and $m_{\gamma_N} = \frac{1}{N} \sum_{i=1}^N K(\cdot, x_i)$. For the second term, we obtain by Lemma 3 that $\nabla_{x_i} m_{\gamma_N} = \frac{1}{N} \nabla_{x_i} K(\cdot, x_i)$. Next, we apply the chain rule, Corollary 14 and the derivative reproducing property of $\partial_j K(\cdot, x_i)$ to get

$$N \nabla_{x_i} D_N(x) = \left(\langle \hat{p}_{\gamma_N}, \partial_j K(\cdot, x_i) \rangle_{\mathcal{H}_K} \right)_{j=1}^d = \nabla \hat{p}_{\gamma_N}(x_i).$$

Consequently, we obtain $\partial_t \gamma_N - \operatorname{div}(\gamma_N \nabla \hat{p}_{\gamma_N}) = 0$ as required. \square

Remark 23 (Consistent discretization). *An advantage of the regularized f -divergences $D_{\nu, f}^\lambda$, $\nu \in \mathcal{P}_2(\mathbb{R}^d)$, is that $D_{\nu, f}^\lambda(\mu) < \infty$ for any $\mu \in \mathcal{P}_2(\mathbb{R}^d)$ (even if $D_{\nu, f}(\mu) = \infty$). This is important when approximating the Wasserstein gradient flow of the functional $D_{\nu, f}$ starting in $\mu_0 \in \operatorname{dom}(D_{\nu, f})$ numerically with gradient flows starting in empirical measures $\mu_{0, N} = \frac{1}{N} \sum_{i=1}^N \delta_{x_i(0)}$. Since $\mu_{0, N}$ might not be in $\operatorname{dom}(D_{\nu, f})$, we choose $(\lambda_N)_{N \in \mathbb{N}}$ with $\lim_{N \rightarrow \infty} \lambda_N = 0$ such that $\sup_{N \in \mathbb{N}} D_{\nu, f}^{\lambda_N}(\mu_{0, N}) < \infty$. Then, as shown in Corollary 13(i), the functionals $D_{\nu, f}^{\lambda_N}$ Mosco converge to $D_{\nu, f}$. If we have a uniform lower bound on their convexity-modulus along generalized geodesics, then [4, Thm. 11.2.1] implies that the Wasserstein gradient flows of $D_{\nu, f}^{\lambda_N}$ starting in $\mu_{0, N}$ converge locally uniformly in $[0, \infty)$ to the flow of $D_{\nu, f}$ starting in μ_0 . Whether such a lower bound exists is so far an open question. In Theorem 19, we only established a lower bound on the weak convexity modulus of $D_{\nu, f}^{\lambda_N}$ which scales as $1/\lambda_N$. A similar convergence result was recently established in [43] for regularization with the Wasserstein distance W_2 instead of the MMD d_K . However, their proof cannot be directly extended to our setting.*

5 Computation of Flows for Empirical Measures

In this section, we are interested in the Wasserstein gradient flows γ of $D_{f,\nu}^\lambda$ with initial measure (40) and target measure $\nu = \frac{1}{M} \sum_{j=1}^M \delta_{y_j}$. For the KL divergence, such flows were considered in [27] under the name KALE flows. The Euler forward discretization of the Wasserstein gradient flow (41) with step size $\tau > 0$ is given by the sequence $(\gamma_n)_{n \in \mathbb{N}} \subset \mathcal{P}_2(\mathbb{R}^d)$ defined by

$$\gamma_{n+1} := (\text{id} - \tau \nabla \hat{p}_n) \# \gamma_n,$$

where \hat{p}_n maximizes the dual formulation (22) of $D_{\nu,f}^\lambda(\gamma_n)$. Since the push-forward of an empirical measure by a measurable map is again an empirical measure with the same number of particles, we have that

$$\gamma_n = \frac{1}{N} \sum_{i=1}^N \delta_{x_i^{(n)}},$$

where

$$x_i^{(n+1)} = x_i^{(n)} - \tau \nabla \hat{p}_n(x_i^{(n)}), \quad i = 1, \dots, N. \quad (42)$$

Since both γ_n and ν are empirical measures, the dual problem (22) for \hat{p}_n becomes

$$\hat{p}_n = \arg \max_{\substack{p \in \mathcal{H}_K \\ p(\mathbb{R}^d) \subseteq \text{dom}(f^*)}} \left\{ \frac{1}{N} \sum_{i=1}^N p(x_i^{(n)}) - \frac{1}{M} \sum_{j=1}^M f^*(p(y_j)) - \frac{\lambda}{2} \|p\|_{\mathcal{H}_K}^2 \right\}. \quad (43)$$

5.1 Discretization Based on Representer Theorem

If $f'_\infty = \infty$ or $\text{supp}(\nu) = \mathbb{R}^d$, then the constraint $p(\mathbb{R}^d) \subset \text{dom}(f^*)$ in (43) becomes superfluous. By the representer theorem [71], the solution of (43) is of the form

$$\hat{p}_n = \sum_{k=1}^{M+N} b_k^{(n)} K(\cdot, z_k^{(n)}), \quad b^{(n)} := (b_k^{(n)})_{k=1}^{M+N} \in \mathbb{R}^{M+N}, \quad (44)$$

where

$$(z_1^{(n)}, \dots, z_{N+M}^{(n)}) = (y_1, \dots, y_M, x_1^{(n)}, \dots, x_N^{(n)}) \in \mathbb{R}^{d \times (M+N)}.$$

We denote the associated kernel matrix by $K^{(n)} := (K(z_i^{(n)}, z_j^{(n)}))_{i,j=1}^{M+N}$.

If $f'_\infty < \infty$, we cannot drop the constraint $p(\mathbb{R}^d) \subset \overline{\text{dom}(f^*)}$ in (22) to apply the representer theorem. The situation is similar for the primal problem (14), where the condition $f'_\infty < \infty$ entails that we have to consider measures μ that are not absolutely continuous with respect to the (empirical) target ν . In the following, we provide a condition under which computing \hat{p}_n for (43) reduces to a tractable finite-dimensional problem. To simplify the notation, we omit the index n and use the shorthand $L(p) = \mathbb{E}_\mu[p] - \mathbb{E}_\nu[f^* \circ p] - \frac{\lambda}{2} \|p\|_{\mathcal{H}_K}^2$ for the objective in (22).

Lemma 24. *Let f be an entropy function with $f'_\infty \in (0, \infty)$. If $\mu, \nu \in \mathcal{M}_+(\mathbb{R}^d)$ and $\lambda > 2d_K(\mu, \nu)\sqrt{\phi(0)}/f'_\infty$, then*

$$\arg \max_{\substack{p \in \mathcal{H}_k \\ p(\mathbb{R}^d) \subseteq \text{supp}(f^*)}} L(p) = \arg \max_{\|p\|_{\mathcal{H}_K} < \frac{f'_\infty}{\sqrt{\phi(0)}}} L(p).$$

If μ, ν are empirical measures with $Z = \text{supp}(\mu) \cup \text{supp}(\nu)$, then the solution \hat{p} of the discrete problem (43) has a finite representation of the form (44).

Proof. First, we introduce shorthand notations for the feasible sets

$$C := \{p \in \mathcal{H}_K : p(\mathbb{R}^d) \subseteq \overline{\text{dom}(f^*)}\} \quad \text{and} \quad X := \left\{p \in \mathcal{H}_K : \|p\|_{\mathcal{H}_K} < \frac{f'_\infty}{\sqrt{\phi(0)}}\right\}.$$

It holds for any $p \in X$ that $\|p\|_\infty \leq \sqrt{\phi(0)}\|p\|_{\mathcal{H}_K} < f'_\infty$, which implies $X \subseteq C$. By (23), the maximizer \hat{p} of (22) satisfies $\|\hat{p}\|_{\mathcal{H}_K} \leq \frac{2}{\lambda}d_K(\mu, \nu)$. For $\lambda > 2d_K(\mu, \nu)\sqrt{\phi(0)}/f'_\infty$, we get $\hat{p} \in X$ due to $\|\hat{p}\|_{\mathcal{H}_K} \leq \frac{2}{\lambda}d_K(\mu, \nu) < f'_\infty/\sqrt{\phi(0)}$. Since $X \subseteq C$, we get that \hat{p} maximizes L over X . This proves the first claim.

For the second part, consider the parameterization $\Psi: \mathcal{H}_K \rightarrow X$ with $\Psi(0) := 0$ and $\Psi(p) := \frac{p}{\|p\|}\psi(\|p\|)$ otherwise, where $\psi: [0, \infty) \rightarrow [0, \frac{f'_\infty}{\phi(0)})$ is given by

$$\psi(t) = \frac{2f'_\infty}{\pi\sqrt{\phi(0)}} \arctan(t).$$

The bijectivity of \arctan directly implies the bijectivity of Ψ . Hence, the reparameterized problem $\arg \max_{q \in \mathcal{H}_K} L(\Psi(q))$ has the unique maximizer $\hat{q} = \Psi^{-1}(\hat{p})$. Since $\hat{q} \in \mathcal{H}_K$, we can decompose \hat{q} as $\hat{q} = \hat{s} + \hat{r}$, where $\hat{s} \in \text{span}\{K(\cdot, z) : z \in Z\}$ and $\hat{r} \in \text{span}\{K(\cdot, z) : z \in Z\}^\perp$. Then, for all $z \in Z$ we get that

$$\hat{q}(z) = \langle \hat{q}, K(\cdot, z) \rangle = \langle \hat{s} + \hat{r}, K(\cdot, z) \rangle = \langle \hat{s}, K(\cdot, z) \rangle = \hat{s}(z).$$

Hence, it holds that

$$\begin{aligned} L(\Psi(\hat{q})) &= \mathbb{E}_\mu[\Psi(\hat{q})] - \mathbb{E}_\nu[f^* \circ \Psi(\hat{q})] - \frac{\lambda}{2} \|\Psi(\hat{q})\|_{\mathcal{H}_K}^2 \\ &= \frac{1}{|\text{supp}(\mu)|} \sum_{z \in \text{supp}(\mu)} \Psi(\hat{s}(z)) - \frac{1}{|\text{supp}(\nu)|} \sum_{z \in \text{supp}(\nu)} f^* \circ \Psi(\hat{s}(z)) - \frac{\lambda}{2} \|\Psi(\hat{q})\|_{\mathcal{H}_K}^2 \\ &= \mathbb{E}_\mu[\Psi(\hat{s})] - \mathbb{E}_\nu[f^* \circ \Psi(\hat{s})] - \frac{\lambda}{2} \|\Psi(\hat{q})\|_{\mathcal{H}_K}^2 \end{aligned}$$

Now, $\|\Psi(\hat{q})\|_{\mathcal{H}_K} = \psi(\|\hat{q}\|_{\mathcal{H}_K})$, $\|\hat{q}\|_{\mathcal{H}_K}^2 = \|\hat{s}\|_{\mathcal{H}_K}^2 + \|\hat{r}\|_{\mathcal{H}_K}^2$ and the strict monotonicity of Ψ^2 imply

$$\begin{aligned} L(\Psi(\hat{q})) &= \mathbb{E}_\mu[\Psi(s)] - \mathbb{E}_\nu[f^* \circ \Psi(\hat{s})] - \frac{2\lambda(f'_\infty)^2}{(\pi\sqrt{\phi(0)})^2} \arctan\left(\sqrt{\|\hat{s}\|_{\mathcal{H}_K}^2 + \|\hat{r}\|_{\mathcal{H}_K}^2}\right)^2 \\ &\leq \mathbb{E}_\mu[\Psi(\hat{s})] - \mathbb{E}_\nu[f^* \circ \Psi(\hat{s})] - \frac{2\lambda(f'_\infty)^2}{(\pi\sqrt{\phi(0)})^2} \arctan(\|\hat{s}\|_{\mathcal{H}_K})^2 = L(\Psi(\hat{s})). \end{aligned}$$

Hence, we must have $\hat{q} = \hat{s}$. This directly implies $\hat{p} = \Psi(\hat{q}) \in \text{span}\{K(\cdot, z) : z \in Z\}$, which means that we can write $\hat{p} = \sum_{z \in Z} b_z K(\cdot, z)$ and $b \in \mathbb{R}^Z$. \square

5.2 Numerical Implementation Details

Recall that both for infinite and finite recession constant (see Lemma 24), the solution \hat{p}_n to the dual problem has the representation

$$\hat{p}_n = \sum_{k=1}^{N+M} b_k^{(n)} K(\cdot, z_k^{(n)}).$$

To determine the coefficients $b^{(n)} = (b_k^{(n)})_{k=1}^{M+N}$, we look instead at the primal problem (21), which by Corollary 10 has a solution of the form

$$\hat{g}_n = m_{\gamma_n} - \lambda \hat{p}_n = \sum_{k=1}^{M+N} \beta_k^{(n)} K(\cdot, z_k^{(n)}) = m_{\hat{\sigma}_n}, \quad \hat{\sigma}_n := \sum_{k=1}^{M+N} \beta_k^{(n)} \delta_{z_k^{(n)}}, \quad (45)$$

with the non-negative coefficients

$$\beta_k^{(n)} := \begin{cases} -\lambda b_k^{(n)}, & \text{if } k \in \{1, \dots, M\} \\ \frac{1}{N} - \lambda b_k^{(n)}, & \text{if } k \in \{M+1, \dots, M+N\}. \end{cases}$$

Hence, to compute $b^{(n)}$, we can minimize the primal objective only with respect to the coefficients $\beta^{(n)}$, which results in the objective

$$J(\beta^{(n)}) = D_{f,\nu}(\hat{\sigma}_n) + \frac{1}{2\lambda} \|m_{\hat{\sigma}_n} - m_{\gamma_n}\|_{\mathcal{H}_K}^2. \quad (46)$$

With the change of variables $q^{(n)} := -\lambda M b^{(n)} \in \mathbb{R}^{N+M}$, we get $\frac{d\hat{\sigma}_n}{d\nu}(z_k^{(n)}) = q_k^{(n)}$ for $k \in \{1, \dots, M\}$ and $\hat{\sigma}_n^s(\mathbb{R}^d) = 1 + \frac{1}{M} \sum_{k=M+1}^{M+N} q_k^{(n)}$. Plugging this into (46) yields

$$\begin{aligned} J(q^{(n)}) &= \int_{\mathbb{R}^d} f \circ \frac{d\hat{\sigma}_n}{d\nu} d\nu + f'_\infty \hat{\sigma}_n^s(\mathbb{R}^d) + \frac{1}{2\lambda M^2} (q^{(n)})^\top K^{(n)} q^{(n)} \\ &= \frac{1}{M} \sum_{k=1}^M f(q_k^{(n)}) + \frac{f'_\infty}{M} \left(M + \sum_{k=M+1}^{M+N} q_k^{(n)} \right) + \frac{1}{2\lambda M^2} (q^{(n)})^\top K^{(n)} q^{(n)}. \end{aligned} \quad (47)$$

For many kernels like the inverse multiquadric or the Gaussian, $K^{(n)}$ is positive definite, so that J is strongly convex.

The constraint $\beta^{(n)} \geq 0$ translates into the constraints

$$q_k^{(n)} = -\lambda b_k^{(n)} M \begin{cases} \geq 0, & k \in \{1, \dots, M\}, \\ = \beta_k^{(n)} - \frac{M}{N} \geq -\frac{M}{N}, & k \in \{M+1, \dots, M+N\}. \end{cases}$$

If $f'_\infty = \infty$, then $q_{k+M}^{(n)} = -\frac{M}{N}$ for $k \in \{1, \dots, N\}$. Hence, we only need to optimize over $(q_k^{(n)})_{k=1}^M$ and consider a reduced objective J instead. Given the optimal coefficients $\hat{q}^{(n)}$, the update step (42) becomes

$$x_j^{(n+1)} = x_j^{(n)} + \frac{\tau}{\lambda M} \sum_{k=1}^{M+N} \hat{q}_k^{(n)} \nabla K(\cdot, z_k^{(n)})(x_j^{(n)}), \quad j \in \{1, \dots, N\}. \quad (48)$$

Now, we detail the computation of $\hat{q}^{(n)}$ based on a forward-backward splitting algorithm. This requires the proximal mapping prox_f of f .^{*} For $f'_\infty < \infty$, we decompose J from (47) into the proper, convex and lower semicontinuous function

$$h_1: \mathbb{R}^{M+N} \rightarrow [0, \infty], \quad q \mapsto \frac{1}{M} \sum_{k=1}^M f(q_k) + \sum_{k=M+1}^{M+N} \iota_{[-\frac{M}{N}, \infty)}(q_k)$$

and the smooth function

$$h_2: \mathbb{R}^{M+N} \rightarrow \mathbb{R}, \quad q \mapsto f'_\infty \left(1 + \frac{1}{M} \sum_{k=1}^N q_{M+k} \right) + \frac{1}{2\lambda M^2} q^T K q$$

with Lipschitz continuous gradient

$$\nabla h_2(q) = \frac{f'_\infty}{M} \begin{bmatrix} 0_M \\ \mathbf{1}_N \end{bmatrix} + \frac{1}{\lambda M^2} K q.$$

If $f'_\infty = \infty$, we decompose J into

$$\begin{aligned} \tilde{h}_1: \mathbb{R}^M &\rightarrow \mathbb{R}, & q &\mapsto \frac{1}{M} \sum_{k=1}^M f(q_k), \\ \tilde{h}_2: \mathbb{R}^M &\rightarrow \mathbb{R}, & q &\mapsto \frac{1}{2\lambda M^2} q^T K_{yy} q - \frac{1}{\lambda M N} \mathbf{1}_N^T K_{xy}^{(n)} q + \frac{1}{2\lambda N^2} \mathbf{1}_N^T K_{xx}^{(n)} \mathbf{1}_N. \end{aligned}$$

^{*}We provide prox_f in closed form for several entropies f in Table 3. For the others, we employ a naive derivative-free method to solve the one-dimensional strongly convex problem defining prox_f .

Algorithm 1: FISTA for solving (22) related to $D_{f,\nu}^\lambda(\mu)$ if $f'_\infty = \infty$

Data: $q_0 \in \mathbb{R}^M$, $t_0 = 1$

Result: Approximate minimizer q^* of J

for $k = 0, \dots$ *until convergence* **do**

$$\left| \begin{array}{l} t_{k+1} \leftarrow \frac{1}{2}(1 + \sqrt{1 + 4t_k^2}); \\ z^{(k)} \leftarrow q^{(k)} + \frac{1}{t_{k+1}}(t_k - 1)(q^{(k)} - q^{(k-1)}); \\ q_j^{(k+1)} \leftarrow \text{prox}_{\frac{\lambda M}{\|K_{yy}\|_2}} f \left(\left(\text{id} - \frac{1}{\|K_{yy}\|_2} K_{yy} \right) z_j^{(k)} + \frac{1}{\lambda M N} (K_{xy}^{(n)})^\top \mathbf{1}_N \right); \end{array} \right.$$

end

Algorithm 2: FISTA for solving (22) related to $D_{f,\nu}^\lambda(\mu)$ if $f'_\infty < \infty$

Data: $q_0 \in \mathbb{R}^{M+N}$, $t_0 = 1$

Result: Approximate minimizer q^* of J

for $k = 0, \dots$ *until convergence* **do**

$$\left| \begin{array}{l} t_{k+1} \leftarrow \frac{1}{2}(1 + \sqrt{1 + 4t_k^2}); \\ z^{(k)} \leftarrow q^{(k)} + \frac{1}{t_{k+1}}(t_k - 1)(q^{(k)} - q^{(k-1)}); \\ q_j^{(k+1)} \leftarrow \text{prox}_{\frac{\lambda M}{\|K\|_2}} f \left(\left(\left(\text{id} - \frac{1}{\|K\|_2} K \right) z^{(k)} \right)_j \right), \quad j = 1, \dots, M; \\ q_{M+j}^{(k+1)} \leftarrow \max \left(-\frac{M}{N}, \left(\left(\text{id} - \frac{1}{\|K\|_2} K \right) z^{(k)} \right)_{M+j} - f'_\infty \frac{\lambda M}{\|K\|_2} \right), \quad j = 1, \dots, N; \end{array} \right.$$

end

The gradient of \tilde{h}_2 reads

$$\nabla \tilde{h}_2(q) = \frac{1}{\lambda M^2} K_{yy} q - \frac{1}{\lambda M N} (K_{xy}^{(n)})^\top \mathbf{1}_N.$$

Since h_1 and \tilde{h}_1 are separable, the same holds for their proximal operators. The FISTA [9] iterations in Algorithm 1 and 2, respectively, converge to the unique minimizer q^* of J . FISTA has the optimal $O(k^{-2})$ convergence rate, meaning that $J(q^{(k)}) - J(q^*) \leq \frac{2L}{(k+1)^2} \|x^{(0)} - x^*\|_2^2$. Since the proximal operator in Algorithm 1 is independent of the particles x_j , we can use the same approximation throughout.

6 Numerical Results

In this section, we use three target measures from the literature to compare how fast the discrete Wasserstein gradient flow (WGF) (48) for different $D_{f,\nu}^\lambda$ converge[†]. We always choose $N = M = 900$ particles. Further, we use the inverse multiquadric kernel from Remark 2. We focus on the Tsallis- α divergence for $\alpha \geq 1$ because the corresponding entropy function is differentiable on the interior of its domain and $f'_\infty = \infty$. Other choices are covered in the code repository. For $\alpha \geq 1$, the Tsallis- α divergence $D_{f_\alpha}(\mu | \nu)$ between $\mu, \nu \in \mathcal{P}(\mathbb{R}^d)$ with $\mu \ll \nu$ reads

$$D_{f_\alpha}(\mu | \nu) = \frac{1}{\alpha - 1} \left(\int_{\mathbb{R}^d} \left(\frac{d\mu}{d\nu}(x) \right)^\alpha d\nu(x) - 1 \right).$$

In our experiments, the commonly used KL divergence (corresponding to the limit for $\alpha \searrow 1$) is outperformed in terms of convergence speed if α is moderately larger than one. We always observed sublinear convergence to the target ν in terms of functional values. This matches the rate proven in [27, Prop. 3] (the same proof is possible for any f -divergence) under an a priori boundedness assumption, which, however, is never fulfilled if μ and ν have disjoint supports. We also observe fast empirical convergence in terms of the MMD and the Wasserstein distance.

Three rings target First, we consider the three rings target from [27, Fig. 1]. Our simulations are provided in Figure 1. The starting point μ_0 of the flow are samples from a normal distribution with variance $s^2 = 2 \times 10^{-3}$ around the leftmost point on the rightmost circle. Further, we choose the kernel width $\sigma^2 = 5 \times 10^{-2}$, regularization parameter $\lambda = 10^{-2}$, and step size $\tau = 10^{-3}$.

For larger α , the particles advance faster towards the leftmost circle in the beginning, and accordingly, the MMD decreases the fastest; see also Figure 2. On the other hand, for too large α , there are more outliers (points that are far away from the rings) at the beginning of the flow. Even at $t = 50$, some of them remain between the rings, which contrasts our observations for smaller α . This is also reflected by the fact that the MMD and W_2 values plateau for these values of α before they finally converge to zero. The “sweet spot” for α seems to be $\alpha \in [3, 4]$ since then the MMD and W_2 drop below 10^{-9} the fastest. For the first few iterations, the MMD values are monotone with respect to α : the lower curve is the one belonging to $\alpha = 7.5$, the one above belongs to $\alpha = 5$, and the top one belongs to $\alpha = 1$. For the last time steps, this order is nearly identical. If $\alpha \in \{10, 50, 100, 500\}$, then the flow behaves even worse in the sense that the plateau phases becomes longer, i.e., both the W_2 and the squared MMD loss converge to 0 even slower.

Neal’s cross target Inspired by [86, Fig. 1f], the target ν comprises four identical versions of Neal’s funnel, each rotated by 90 degrees about the origin, see Figure 3. We

[†]The code is available at https://github.com/ViktorAJStein/Regularized_f_Divergence_Particle_Flows. We use pytorch [57] to benefit from GPU parallelization.

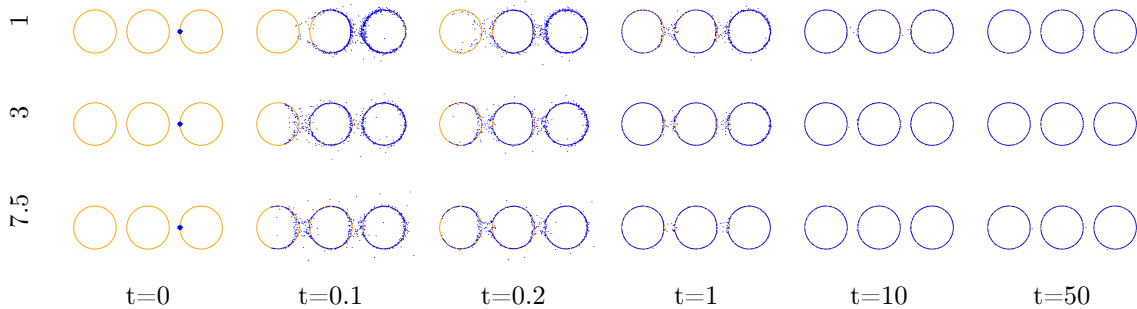


Figure 1: WGF of the regularized Tsallis- α divergence $D_{f_\alpha, \nu}^\lambda$ for $\alpha \in \{1, 3, 7.5\}$.

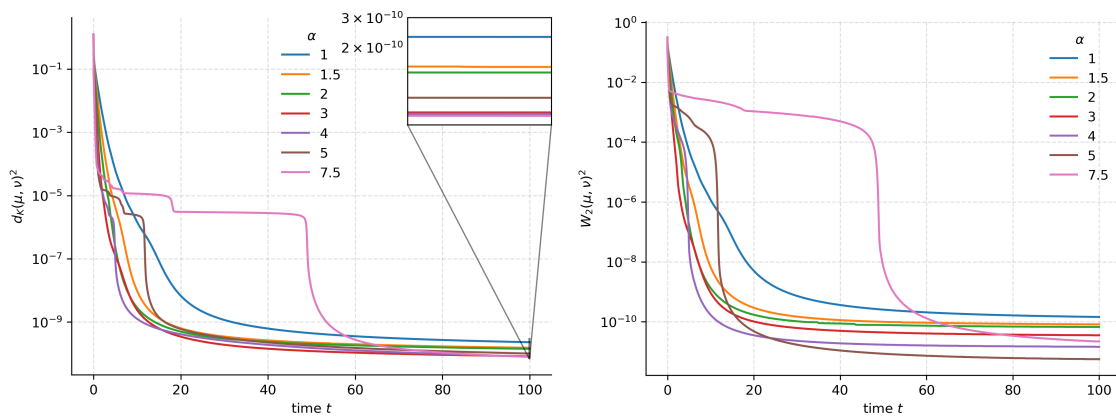


Figure 2: Comparison of squared MMD (**left**) and W_2 distance (**right**) along the flow for different α , where ν is the three circles target. Note the logarithmic axis.

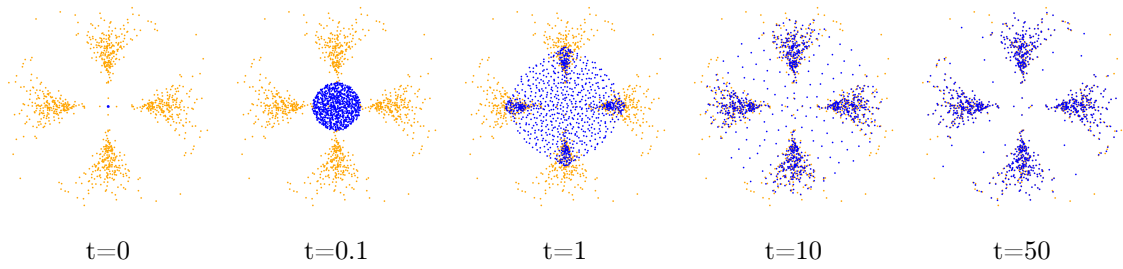


Figure 3: WGF of the regularized Tsallis- α divergence $D_{f_{7.5,\nu}}^\lambda$ for Neals cross.

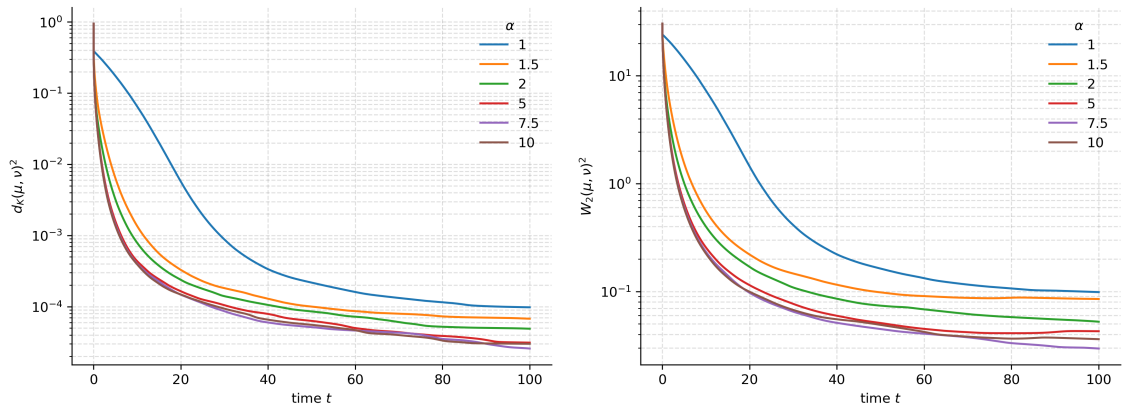


Figure 4: Comparison of the flow for $D_{f_{\alpha,\nu}}^\lambda$, where ν is Neal's cross. We depict the squared MMD (**left**) and Wasserstein distance (**right**) to ν for different α .

generate the samples $\{(x_{1,k}, x_{2,k})\}_{k=1}^N$ by drawing normally distributed samples $x_{2,k} \sim \mathcal{N}(7.5, 2)$ and $x_{1,k} \sim \mathcal{N}(0, e^{\frac{1}{3}x_{2,k}})$, where $\mathcal{N}(m, s^2)$. For our simulations, we choose $\alpha = 7.5$, $\lambda = 10^{-2}$, $\tau = 10^{-3}$ and $\sigma^2 = 0.25$.

We observe that the particles (blue) are pushed towards the regions with a high density of target particles (orange) and that the low-density regions at the ends of the funnel are not matched exactly. Since the target ν is usually obtained by drawing samples from a distribution, this behavior is acceptable. Figure 4 shows that for $\alpha = 1$ the gradient flow with respect to $D_{f_{\alpha}, \nu}^{\lambda}$ recovers the target slower, both in terms of the MMD or the W_2 metric and that $\alpha = 7.5$ performs best.

Bananas target This experiment is inspired by a talk from Aude Genevay[‡], see Figure 5. The target ν is multimodal and the “connected components” of its support are far apart. Additionally, the chosen initial measure does not take the properties of $\text{supp}(\nu)$ into account. Still, we observe the convergence of the particles to the target ν . We also observe a mode-seeking behavior: the particles concentrate near the mean of the right “banana” first, which is even more pronounced for the left “banana” at later time points.

Since the parameter λ penalizes the disjoint support condition, we choose λ to be higher than for the other targets, namely $\lambda = 1$, so that the particles are encouraged to “jump” from one mode to another. Further, we choose $\tau = 10^{-1}$, $\sigma = 2 \times 10^{-2}$ and $\alpha = 3$ for the simulations. Empirically, we observed that the value of α makes no difference though.

Finite recession constant and annealing Lastly, in Figures 6 and 7, we show that the three rings target is also well recovered for entropy functions with finite recession constant. To illustrate the convergence of our procedure, we first choose the total variation entropy function, $\tau = 10^{-3}$ and the kernel width $\sigma = 5 \times 10^{-2}$. According to Lemma 24, we choose $\lambda = 2.25$. As a second example, we choose the $\frac{1}{2}$ -Tsallis entropy function, $\tau = 10^{-3}$ and the kernel width $\sigma = 5 \times 10^{-2}$ as well as $\lambda = 2.25$ (so that Lemma 24 applies).

Since smaller λ leads to better target recovery, we use an annealing heuristic (similar to [19]): Ultimately, we want to sample for the target distribution. Hence, we reduce the value of λ along the flow. This is justified as follows. For the Wasserstein gradient flow $(\gamma_t)_t$ with respect to $D_{f, \nu}^{\lambda}$ for a fixed λ , we expect that $D_f^{\lambda}(\gamma_t, \nu) \rightarrow 0$ as $t \rightarrow \infty$. Then, by Corollary 12(3), the same holds for $d_K(\gamma_t, \nu)$, see also Figures 2 and 4 for empirical evidence. Based on Lemma 24, we can thus reduce the value of λ along the flow while maintaining the finite-dimensional minimization problem. In this last example, we divide the value of λ by five three times, namely at $t \in \{5, 10, 20\}$. This indeed improved the convergence.

7 Conclusions and Limitations

We have proven that the proposed MMD regularized f -divergences are M -convex along generalized geodesics, and calculated their gradients. This ensures the existence and unique-

[‡]MIFODS Workshop on Learning with Complex Structure 2020, see https://youtu.be/TFdIJib_zEA?si=B3fsQkfmjea2HCA5.

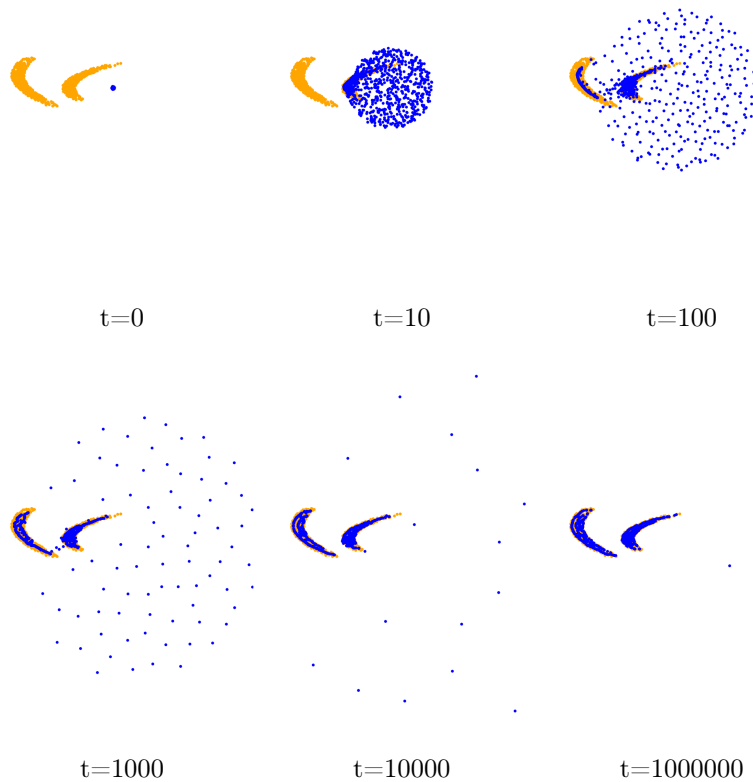


Figure 5: WGF of the regularized Tsallis-3 divergence $D_{f_{3,\nu}}^\lambda$ with the bananas target.

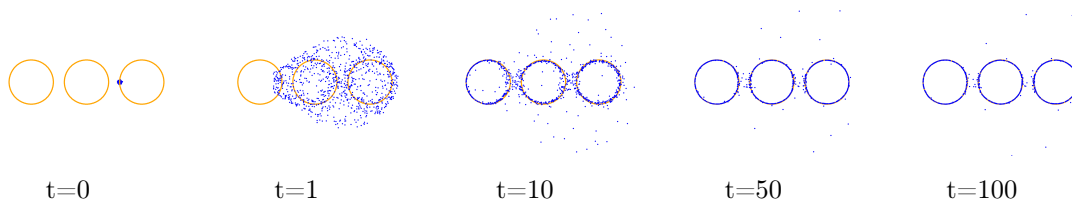


Figure 6: WGF of the regularized TV divergence $D_{f_{TV,\nu}}^\lambda$ with the three rings target.

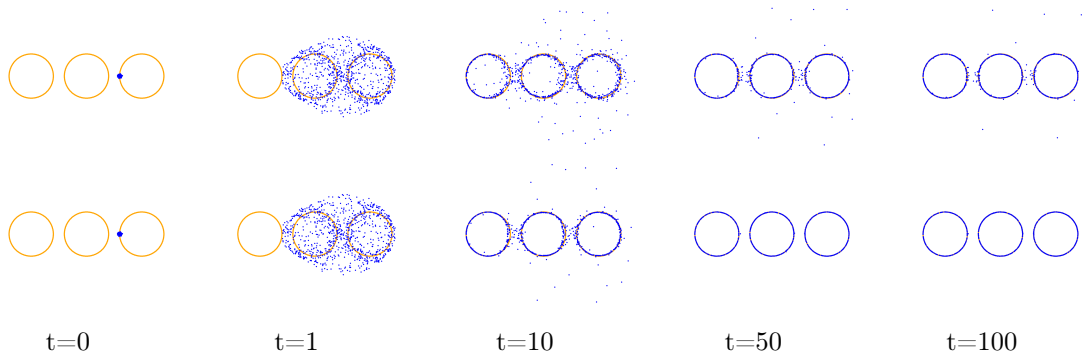


Figure 7: WGF of the regularized $\frac{1}{2}$ -Tsallis divergence $D_{f_{\frac{1}{2},\nu}}^\lambda$ without (top) and with annealing (bottom), where ν is the three rings target.

ness of the associated Wasserstein gradient flows. When considering particle flows for f -divergences with $f'_\infty = \infty$ or if the regularization parameter λ is chosen in a certain way, each forward Euler step reduces to solving a finite-dimensional, strongly convex optimization problem. Proving the observed sublinear convergence rate of the flows is subject to future work.

Further, we would like to extend this paper’s theory to non-differentiable kernels such as the Laplace kernel, i.e., the Matérn- $\frac{1}{2}$ kernel, and to non-bounded kernels like Coulomb kernels or Riesz kernels, which are of interest, e.g., in generative modeling [32, 33] and image dithering [25].

Recently, we became aware of [20], where they consider infimal convolution functionals as smoother loss functions in generative adversarial networks. In particular, the infimal convolution of the MMD arising from the Gaussian kernel and convex functions appears promising. Potentially, our results can contribute in this direction, which is also in the spirit of [12, 26, 74].

Acknowledgments

We thank the anonymous reviewer for pointing us to the tight variational formulation. V.S. and G.S. gratefully acknowledge funding from the BMBF project “VI-Screen” with number 13N15754. V.S. extends his gratitude to J.-F. Bercher for making the paper [82] available.

References

- [1] R. Agrawal and T. Horel. Optimal bounds between f -divergences and Integral Probability Metrics. *J. Mach. Learn. Res.*, 22(1), jan 2021.

- [2] S. M. Ali and S. D. Silvey. A general class of coefficients of divergence of one distribution from another. *J. R. Stat. Soc. Ser. B. Stat. Methodol.*, 28(1):131–142, 1966.
- [3] L. Ambrosio, N. Fusco, and D. Pallara. *Functions of bounded variation and free discontinuity problems*. Oxford Mathematical Monographs. Oxford University Press, 2000.
- [4] L. Ambrosio, N. Gigli, and G. Savaré. *Gradient flows: in metric spaces and in the space of probability measures*. Springer Science & Business Media, 2 edition, 2008.
- [5] A. Andrieu, N. Farchmin, P. Hagemann, S. Heidenreich, V. Soltwisch, and G. Steidl. Invertible neural networks versus MCMC for posterior reconstruction in grazing incidence X-ray fluorescence. In *International Conference on Scale Space and Variational Methods in Computer Vision*, pages 528–539, Virtual event, May 16–20 2021. Springer.
- [6] M. Arbel, L. Zhou, and A. Gretton. Generalized energy based models. In *International Conference on Learning Representations*, Virtual event, May 3–7 2021.
- [7] H. Bauschke and P. Combettes. *Convex Analysis and Monotone Operator Theory in Hilbert Spaces*. CMS Books in Mathematics. Springer Cham, 2nd edition, 2017.
- [8] A. Beck and M. Teboulle. Mirror descent and nonlinear projected subgradient methods for convex optimization. *Operations Research Letters*, 31(3):167–175, 2003.
- [9] A. Beck and M. Teboulle. A fast iterative shrinkage-thresholding algorithm for linear inverse problems. *SIAM Journal on Imaging Sciences*, 2(1):183–202, 2009.
- [10] F. Beier, J. von Lindheim, S. Neumayer, and G. Steidl. Unbalanced multi-marginal optimal transport. *J. Math. Imaging Vision*, 65(3):394–413, 2023.
- [11] P. Billingsley. *Convergence of probability measures*. John Wiley & Sons, 2 edition, 2013.
- [12] J. Birrell, P. Dupuis, M. A. Katsoulakis, Y. Pantazis, and L. Rey-Bellet. (f, Γ) -divergences: Interpolating between f -divergences and integral probability metrics. *J. Mach. Learn. Res.*, 23(39):1–70, 2022.
- [13] D. M. Blei, A. Kucukelbir, and J. D. McAuliffe. Variational inference: A review for statisticians. *J. Amer. Statist. Assoc.*, 112(518):859–877, 2017.
- [14] D. E. Boekee. *A generalization of the Fisher information measure*. PhD thesis, Delft University, 1977.
- [15] K. M. Borgwardt, A. Gretton, M. J. Rasch, H.-P. Kriegel, B. Schölkopf, and A. J. Smola. Integrating structured biological data by kernel maximum mean discrepancy. *Bioinformatics*, 22(14):e49–e57, 07 2006.

- [16] J. M. Borwein and A. S. Lewis. Partially-finite programming in L_1 and the existence of maximum entropy estimates. *SIAM J. Optim.*, 3(2):248–267, 1993.
- [17] A. Braides. A Handbook of Γ -convergence. In M. Chipot, editor, *Handbook of Differential Equations: Stationary Partial Differential Equations*, volume 3, pages 101–213. Elsevier, 2006.
- [18] Z. Chen, A. Mustafi, P. Glaser, A. Korba, A. Gretton, and B. K. Sriperumbudur. (de)-regularized maximum mean discrepancy gradient flow. ArXiv preprint, 2024.
- [19] L. Chizat. Mean-field Langevin dynamics: Exponential convergence and annealing. *J. Mach. Learn. Res.*, 2022, 2022.
- [20] C. Chu, K. Minami, and K. Fukumizu. Smoothness and stability in GANs. In *International Conference on Learning Representations*, Virtual event, Apr 26 – May 1 2020.
- [21] R. M. Corless, G. H. Gonnet, D. E. Hare, D. J. Jeffrey, and D. E. Knuth. On the lambert w function. *Advances in Computational mathematics*, 5:329–359, 1996.
- [22] I. Csiszár. Eine informationstheoretische Ungleichung und ihre Anwendung auf den Beweis der Ergodizität von Markoffschen Ketten. *Magyar. Tud. Akad. Mat. Kutato Int. Kozl.*, 8:85–108, 1964.
- [23] I. Csiszár and J. Fischer. Informationsentfernungen im Raum der Wahrscheinlichkeitsverteilungen. *Magyar. Tud. Akad. Mat. Kutato Int. Kozl.*, 7:159–180, 1962.
- [24] F. Cucker and D. Zhou. *Learning Theory: An Approximation Theory Viewpoint*. Cambridge University Press, 2007.
- [25] M. Ehler, M. Gräf, S. Neumayer, and G. Steidl. Curve based approximation of measures on manifolds by discrepancy minimization. *Found. Comput. Math.*, 21(6):1595–1642, 2021.
- [26] F. Farnia and D. Tse. A convex duality framework for GANs. In *Advances in Neural Information Processing Systems*, volume 31, pages 5248 – 5258, Montréal, Canada, 03.12 - 08.12 2018.
- [27] P. Glaser, M. Arbel, and A. Gretton. KALE flow: A relaxed KL gradient flow for probabilities with disjoint support. In *Advances in Neural Information Processing Systems*, volume 34, pages 8018–8031, Virtual event, 6–14 Dec 2021.
- [28] I. Goodfellow, J. Pouget-Abadie, M. Mirza, B. Xu, D. Warde-Farley, S. Ozair, A. Courville, and Y. Bengio. Generative adversarial nets. In *Advances in Neural Information Processing Systems*, volume 27, Montréal, Canada, 8–13 Dec 2014.

- [29] A. Gretton, K. M. Borgwardt, M. J. Rasch, B. Schölkopf, and A. Smola. A kernel two-sample test. *J. Mach. Learn. Res.*, 13(25):723–773, 2012.
- [30] H. Gu, P. Birmpa, Y. Pantazis, L. Rey-Bellet, and M. A. Katsoulakis. Lipschitz regularized gradient flows and latent generative particles. arXiv preprint arXiv:2210.17230, 2022.
- [31] E. Hellinger. Neue Begründung der Theorie quadratischer Formen von unendlichvielen Veränderlichen. *J. Reine Angew. Math.*, 1909(136):210–271, 1909.
- [32] J. Hertrich, M. Gräf, R. Beinert, and G. Steidl. Wasserstein steepest descent flows of discrepancies with Riesz kernels. *J. Math. Anal. Appl.*, 531(1):127829, 2024.
- [33] J. Hertrich, C. Wald, F. Altekruiger, and P. Hagemann. Generative sliced MMD flows with Riesz kernels. In *International Conference on Learning Representations (ICLR)*, Vienna, Austria, 7 – 11 May 2024.
- [34] J. Hunter and D. Dale. The Matplotlib user’s guide, 2007. Matplotlib 0.90.0 user’s guide.
- [35] H. Jeffreys. An invariant form for the prior probability in estimation problems. *Proc. R. Soc., Lond., Ser. A*, 186(1007):453–461, 1946.
- [36] H. Jeffreys. *Theory of Probability*. Oxford, at the Clarendon Press, 2 edition, 1948.
- [37] M. I. Jordan, Z. Ghahramani, T. S. Jaakkola, and L. K. Saul. An introduction to variational methods for graphical models. *Mach. Learn.*, 37:183–233, 1999.
- [38] R. Jordan, D. Kinderlehrer, and F. Otto. The variational formulation of the Fokker–Planck equation. *SIAM J. Math. Anal.*, 29(1):1–17, 1998.
- [39] P. Kafka, F. Österreicher, and I. Vincze. On powers of f -divergences defining a distance. *Studia Sci. Math. Hungar.*, 26(4):415–422, 1991.
- [40] S. Kesavan. *Functional Analysis*, volume 52. Springer Nature, 2 edition, 2023.
- [41] H. Kremer, N. Y., B. Schölkopf, and J.-J. Zhu. Estimation beyond data reweighting: kernel methods of moments. In *ICML’23: Proceedings of the 40th International Conference on Machine Learning*, volume 202, page 17745–17783, Honolulu, Hawaii, USA, July 23 - 29 2023.
- [42] S. Kullback and R. A. Leibler. On information and sufficiency. *Ann. Math. Stat.*, 22(1):79–86, 1951.
- [43] H. Leclerc, Q. Mérigot, F. Santambrogio, and F. Stra. Lagrangian discretization of crowd motion and linear diffusion. *SIAM J. Numer. Anal.*, 58(4):2093–2118, 2020.

- [44] Y.-H. Li and V. Cevher. Convergence of the exponentiated gradient method with armijo line search. *Journal of Optimization Theory and Applications*, 181(2):588–607, 2019.
- [45] M. Liero, A. Mielke, and G. Savaré. Optimal entropy-transport problems and a new Hellinger–Kantorovich distance between positive measures. *Invent. Math.*, 211(3):969–1117, 12 2017.
- [46] F. Liese and I. Vajda. *Convex Statistical Distances*. Teubner-Texte der Mathematik, 1987.
- [47] J. Lin. Divergence measures based on the Shannon entropy. *IEEE Trans. Inf. Theory*, 37(1):145–151, 1991.
- [48] B. G. Lindsay. Efficiency versus robustness: The case for minimum Hellinger distance and related methods. *Ann. Statist.*, 22(2):1081 – 1114, 1994.
- [49] G. Maso. *An Introduction to Γ -Convergence*. Birkhäuser Boston, MA, 1 edition, 1993.
- [50] K. Muandet, K. Fukumizu, B. Sriperumbudur, and B. Schölkopf. Kernel mean embedding of distributions: A review and beyond. *Found. Trends Mach. Learn.*, 10(1-2):1–141, 2017.
- [51] Y. Nesterov. *Introductory Lectures on Convex Optimization: A Basic Course*, volume 87 of *Applied Optimization*. Springer New York, NY, 1 edition, 2003.
- [52] X. Nguyen, M. J. Wainwright, and M. I. Jordan. Estimating divergence functionals and the likelihood ratio by convex risk minimization. *IEEE Trans. Inf. Theor.*, 56(11):5847–5861, Nov. 2010.
- [53] F. Nielsen and R. Nock. On Rényi and Tsallis entropies and divergences for exponential families. arXiv preprint arXiv:1105.3259, 2011.
- [54] F. Österreicher. The construction of least favourable distributions is traceable to a minimal perimeter problem. *Studia Sci. Math. Hungar.*, 17:341–351, 1982.
- [55] F. Österreicher. On a class of perimeter-type distances of probability distributions. *Kybernetika (Prague)*, 32:389–393, 1996.
- [56] F. Österreicher and I. Vajda. A new class of metric divergences on probability spaces and its applicability in statistics. *Ann. Inst. Statist. Math.*, 55(3):639–653, 2003.
- [57] A. Paszke, S. Gross, F. Massa, A. Lerer, J. Bradbury, G. Chanan, T. Killeen, Z. Lin, N. Gimelshein, L. Antiga, et al. PyTorch: An imperative style, high-performance deep learning library. In *Advances in Neural Information Processing Systems*, volume 32, Vancouver Convention Center, Canada, 8–14 Dec 2019.

- [58] K. Pearson. On the criterion that a given system of deviations from the probable in the case of a correlated system of variables is such that it can be reasonably supposed to have arisen from random sampling. *London Edinburgh Philos. Mag. & J. Sci.*, 50(302):157–175, 1900.
- [59] F. e. a. Pedregosa. Scikit-learn: Machine learning in Python. *Journal of Machine Learning Research*, 12:2825–2830, 2011.
- [60] A.-P. Perkkiö. Conjugates of integral functionals on continuous functions. *J. Math. Anal. Appl.*, 459(1):124–134, 2018.
- [61] G. Plonka, D. Potts, G. Steidl, and M. Tasche. *Numerical Fourier Analysis. Applied and Numerical Harmonic Analysis*. Birkhäuser, second edition, 2023.
- [62] Y. Polyanskiy and Y. Wu. Information theory: From coding to learning. Book draft.
- [63] M. L. Puri and I. Vincze. Measure of information and contiguity. *Statist. Probab. Lett.*, 9(3):223–228, 1990.
- [64] C. E. Rasmussen and C. K. I. Williams. *Gaussian processes for Machine Learning*, volume 1. MIT Press, 2006.
- [65] R. T. Rockafellar. Integrals which are convex functionals. *Pacific J. Math.*, 24(3):525–539, 1968.
- [66] R. T. Rockafellar. Integrals which are convex functionals. II. *Pacific J. Math.*, 39(2):439–469, 1971.
- [67] R. T. Rockafellar and R. J.-B. Wets. *Variational Analysis*, volume 317 of *Grundlehren der mathematischen Wissenschaften*. Springer Berlin, 2009.
- [68] A. Ruderman, M. D. Reid, D. García-García, and J. Petterson. Tighter variational representations of f-divergences via restriction to probability measures. In *ICML’12: Proceedings of the 29th International Conference on Machine Learning*, pages 1155–1162, Edinburgh, Scotland, 26. June - 01. July 2012.
- [69] Rémi Flamary et al. POT: Python optimal transport. *J. Mach. Learn. Res.*, 22(78):1–8, 2021.
- [70] I. Sason and S. Verdú. f -divergence inequalities. *IEEE Transactions on Information Theory*, 62(11):5973–6006, 2016.
- [71] B. Schölkopf, R. Herbrich, and A. J. Smola. A generalized representer theorem. In D. Helmbold and B. Williamson, editors, *Computational Learning Theory*, pages 416–426, Berlin, Heidelberg, 2001. Springer Berlin Heidelberg.

- [72] J. Shawe-Taylor and N. Cristianini. *Kernel Methods for Pattern Analysis*. Cambridge University Press, fourth edition, 2009.
- [73] C.-J. Simon-Gabriel and B. Schölkopf. Kernel distribution embeddings: Universal kernels, characteristic kernels and kernel metrics on distributions. *J. Mach. Learn. Res*, 19(1):1708–1736, 2018.
- [74] J. Song and S. Ermon. Bridging the gap between f-GANs and Wasserstein GANs. In H. D. III and A. Singh, editors, *Proceedings of the 37th International Conference on Machine Learning*, volume 119 of *Proceedings of Machine Learning Research*, pages 9078–9087. PMLR, 13–18 Jul 2020.
- [75] B. Sriperumbudur, K. Fukumizu, and G. Lanckriet. On the relation between universality, characteristic kernels and RKHS embedding of measures. In Y. W. Teh and M. Titterton, editors, *Proceedings of the Thirteenth International Conference on Artificial Intelligence and Statistics*, volume 9 of *Proceedings of Machine Learning Research*, pages 773–780, Chia Laguna Resort, Sardinia, Italy, 13–15 May 2010. PMLR.
- [76] I. Steinwart and A. Christmann. *Support Vector Machines*. Springer Science & Business Media, 2008.
- [77] I. Steinwart and J. Fasciati-Ziegel. Strictly proper kernel scores and characteristic kernels on compact spaces. *Appl. Comput. Harmon. Anal.*, 51:510–542, 2021.
- [78] T. Séjourné, J. Feydy, F.-X. Vialard, A. Trounev, and G. Peyré. Sinkhorn divergences for unbalanced optimal transport. arXiv:1910.12958, 2019.
- [79] D. Terjék. Moreau-Yosida f -divergences. In *International Conference on Machine Learning (ICML)*, pages 10214–10224, Virtual event, Jul 18–24 2021. PMLR.
- [80] C. Tsallis. Generalized entropy-based criterion for consistent testing. *Phys. Rev. E*, 58(2):1442, 1998.
- [81] I. Vajda. On the f -divergence and singularity of probability measures. *Period. Math. Hungar.*, 2(1-4):223–234, 1972.
- [82] I. Vajda. χ^α -divergence and generalized Fisher information. In J. Kozesnik, editor, *Transactions of the Sixth Prague Conference on Information Theory, Statistical Decision Functions and Random Processes, Held at Prague, from September 19 to 25, 1971*, pages 873–886. Czechoslovak Academy of Sciences, Academia Publishing House, 1973.
- [83] T. Vayer and R. Gribonval. Controlling Wasserstein distances by kernel norms with application to compressive statistical learning. *J. Mach. Learn. Res*, 24(149):1–51, 2023.

- [84] I. Vincze. On the concept and measure of information contained in an observation. In J. Gani and V. Rohatgi, editors, *Contributions to Probability*, pages 207–214. Elsevier, 1981.
- [85] H. Wendland. *Scattered Data Approximation*. Cambridge University Press, 2004.
- [86] Z. Xu, N. Chen, and T. Campbell. Mixflows: principled variational inference via mixed flows. In *ICML'23: Proceedings of the 40th International Conference on Machine Learning*, page 38342–38376, Honolulu, Hawaii, USA, July 23 - 29 2023.
- [87] J.-K. You and Y.-H. Li. Two Polyak-type step sizes for mirror descent. arXiv preprint, 2022.
- [88] T.-Y. Zhou, N. Suh, G. Cheng, and X. Huo. Approximation of rkhs functionals by neural networks. ArXiv preprint, 2024.

A Entropy Functions and Their f -Divergences

In Table 1 and 2, we give an extensive overview on entropy functions f together with their recession constants, convex conjugates, and associated f -divergences. The (\star) marks that we were not able to find a closed form for the convex conjugate.

Let us briefly discuss some cases of the f -divergences below:

- The Tsallis-2-divergence is also called χ^2 or Pearson divergence [58]. The Tsallis- $\frac{1}{2}$ -divergence is equal to the Matusita- $\frac{1}{2}$ -divergence and equal to half of the squared Hellinger distance [31]. In the limit $\alpha \nearrow 1$, the Matusita entropy function converges to the TV entropy function.
- For $\alpha \rightarrow 1$, both the power and the Tsallis divergence recover the Kullback-Leibler divergence. However, only the power divergence recovers the reverse Kullback-Leibler divergence for $\alpha \rightarrow 0$, while the Tsallis entropy function converges to 0.
- The $\frac{1}{2}$ -Lindsay divergence is called triangular discrimination or Vincze-Le Cam [84, Eq. (2)] divergence. The Lindsay divergence interpolates between the χ^2 divergence and the reverse χ^2 divergence, which are recovered in the limits $\alpha \searrow 1$ and $\alpha \nearrow 0$, respectively. In the limit $\alpha \rightarrow 1$, the perimeter-type divergence recovers the Jensen-Shannon divergence, and in the limit $\alpha \rightarrow 0$, it recovers $\frac{1}{2}$ times the TV-divergence. The special case $\alpha = \frac{1}{2}$ already appears in [54, p. 342].
- For $\alpha \searrow 1$, Vajda's χ^α divergence becomes the TV-divergence - the only (up to multiplicative factors) f -divergence that is a metric.
- The Marton divergence plays an essential role in the theory of concentration of measures; see [62, Rem. 7.15] and the references therein.
- If $f = \iota_1$, then $D_{f,\nu}^\lambda = \frac{1}{2\lambda} d_K(\cdot, \nu)^2$ recovers the squared MMD.
- Not all functions f listed below fulfill the assumptions of this paper. For example, we require that f has a unique minimizer at 1, which is not true for the last three entropy functions.

Table 1: Entropy functions with recession constants and conjugates.

name	entropy $f(x)$	f'_∞	$f^*(y)$
Tsallis [80], $\alpha \in (0, 1) \cup (1, \infty)$	$\frac{1}{\alpha-1}(x^\alpha - \alpha x + \alpha - 1)$	$\iota_{(0,1)}(\alpha) - \frac{\alpha}{\alpha-1}$	$(\frac{\alpha-1}{\alpha}y+1)^{\frac{\alpha}{\alpha-1}} - 1 + \mathbb{1}_{(0,1)}(\alpha) \cdot \iota_{(-\infty, \frac{\alpha}{1-\alpha})}(y)$
power divergence, $\alpha \in \mathbb{R} \setminus \{0, 1\}$ [45]	$\frac{1}{\alpha(\alpha-1)}(x^\alpha - \alpha x + \alpha - 1)$	$\begin{cases} \infty, & \alpha \geq 1, \\ \frac{1}{1-\alpha}, & \alpha < 1 \end{cases}$	$\begin{cases} \frac{1}{\alpha}((\alpha-1)y+1)^{\frac{\alpha}{\alpha-1}} - \frac{1}{\alpha}, & \text{if } \alpha > 1, \\ g_\alpha(y) + \iota_{(-\infty, \frac{1}{1-\alpha})}(y), & \text{if } 0 < \alpha < 1, \\ g_\alpha(y) + \iota_{(-\infty, \frac{1}{1-\alpha})}(y), & \text{if } \alpha < 0, \end{cases}$ where $g_\alpha(y) := \frac{1}{\alpha}(((\alpha-1)y+1)^{\frac{\alpha}{\alpha-1}} - \frac{1}{\alpha})$
Kullback-Leibler [42]	$x \ln(x) - x + 1$	∞	$e^y - 1$
Jeffreys [35, Eq. 1]	$(x-1) \ln(x)$	∞	$y + 2 + W_0(e^{1-y}) + \frac{1}{W_0(e^{1-y})}$
Vajda's χ^α , $\alpha > 1$ [81, 82]	$ x-1 ^\alpha$	∞	$\begin{cases} y + (\alpha-1) \left(\frac{ y }{\alpha}\right)^{\frac{\alpha}{\alpha-1}}, & \text{if } y \geq -\alpha, \\ -1, & \text{else.} \end{cases}$
equality indicator [10, 78]	$\iota_{\{1\}}$	∞	y
Jensen-Shannon [47]	$x \ln(x) - (x+1) \ln\left(\frac{x+1}{2}\right)$	$\ln(2)$	$\iota_{(-\infty, \ln(2))}(y) - \ln(2 - e^y)$.
α -Lindsay, $\alpha \in [0, 1]$ [48]	$\frac{(x-1)^2}{\alpha+(1-\alpha)x}$	$\frac{1}{1-\alpha}$	$\begin{cases} \infty & \text{if } y > \frac{1}{1-\alpha}, \\ \frac{\alpha(\alpha-1)y - 2\sqrt{(\alpha-1)y+1} + 2}{(\alpha-1)^2} & \text{else.} \end{cases}$
Perimeter-type, $\alpha \in \mathbb{R} \setminus \{0, 1\}$ [55, 56]	$\frac{\text{sgn}(\alpha)}{1-\alpha} \left((x^{\frac{1}{\alpha}} + 1)^\alpha - 2^{\alpha-1}(x+1) \right)$	$\begin{cases} \ln(2), & \alpha = 1, \\ \frac{1}{1-\alpha}(1-2^{\alpha-1}), & \alpha > 0, \\ \frac{1}{2}, & \alpha = 0, \\ \frac{1}{1-\alpha}2^{\alpha-1}, & \alpha < 0. \end{cases}$	$\begin{cases} \frac{y - \frac{\text{sgn}(\alpha)}{1-\alpha} \left(h_\alpha(y)^{\frac{\alpha}{\alpha-1}} - 2^{\alpha-1} \right)}{(\alpha-1)^2} + \frac{\text{sgn}(\alpha)}{1-\alpha} 2^{\alpha-1}, & y < f'_\infty, \\ \frac{1}{1-\alpha}(1-2^{\alpha-1}) + \iota_{(-\infty, 0)}(\alpha), & y = f'_\infty, \\ \infty, & \text{else} \end{cases}$ where $h_\alpha(y) := \frac{1-\alpha}{\text{sgn}(\alpha)}y + 2^{\alpha-1}$
Burg [42]	$-\ln(x) + x - 1$	1	$-\ln(1-y) + \iota_{(-\infty, 1)}(y)$
Symmetrized Tsallis, $s \in (0, 1)$ [23]	$1 + x - (x^s + x^{1-s})$	1	(*)
Matusita $\alpha \in (0, 1)$ [14, Eq. (4.1.30)] [36, p. 158]	$ 1 - x ^\alpha$	1	$(y - y)^{\frac{1}{1-\alpha}} \left(1 - \text{sgn}(y) y ^{\frac{\alpha}{1-\alpha}} \right)^{-\frac{1}{\alpha}} + \iota_{(-\infty, 1)}(y)$
Kafka $\alpha \in (0, 1]$ [63], [39]	$ 1 - x ^{\frac{1}{\alpha}}(1+x)^{\frac{\alpha-1}{\alpha}}$	1	(*)
total variation [10, 78]	$ x-1 $	1	$\begin{cases} \max(-1, y) & \text{if } y \leq 1, \\ \infty & \text{otherwise} \end{cases}$
Marton [62, Rem. 7.15]	$\max(0, 1-x)^2$	0	$\begin{cases} \infty, & \text{if } y > 0, \\ \frac{1}{4}y^2 + y, & \text{if } -2 \leq y \leq 0, \\ -1 & \text{else.} \end{cases}$
Hockey stick [70, Eq. (67)]	$\max(0, 1-x)$	0	$\begin{cases} \max(-1, y) & \text{if } y \leq 0, \\ \infty & \text{otherwise} \end{cases}$
zero [10, 78]	$\iota_{[0, \infty)}$	0	$\iota_{(-\infty, 0)}(y)$

B Regularization of the Tight Variational Formulation

The tight variational formulation of f -divergences [68, 52, 79] is derived as the biconjugate of the restricted objective

$$\tilde{D}_{f,\nu}: \mathcal{M}(\mathbb{R}^d) \rightarrow [0, \infty], \quad \mu \mapsto D_{f,\nu}(\mu) + \delta_{\mathcal{P}(\mathbb{R}^d)}(\mu). \quad (49)$$

This indeed leads to another dual formulation of $D_{f,\nu}$ for $\mu, \nu \in \mathcal{P}(\mathbb{R}^d)$, namely

$$D_{f,\nu}(\mu) = \sup_{g \in Y} \{ \mathbb{E}_\mu[g] - (\tilde{D}_{f,\nu})^*(g) \}, \quad (50)$$

where Y denotes the space of bounded measurable functions. By [1, Prop. 28], the conjugate $(\tilde{D}_{f,\nu})^*$ is determined by the one-dimensional convex problem

$$(\tilde{D}_{f,\nu})^*(g) = \inf \left\{ \int_{\mathbb{R}^d} f^*(g(x) + \lambda) d\nu(x) - \lambda : \lambda + \sup(g) \leq f'_\infty \right\}. \quad (51)$$

This is different than the closed form (19) in the non-tight case. An algorithm to solve (51) is given in [79, Algo. 1]. Sometimes, as for $f = f_{\text{KL}}$, the functional $(\tilde{D}_{f,\nu})^*(g)$ is available in closed form: $(\tilde{D}_{f_{\text{KL}},\nu})^*(g) = \log \left(\int_{\mathbb{R}^d} e^g d\nu \right)$. The dual (50) has proven advantageous towards estimating $D_{f,\nu}$ for $\mu, \nu \in \mathcal{P}(\mathbb{R}^d)$ from samples since the objective in (50) is always larger or equal than the one in the original dual (12).

Given the dual form (22) of regularized f divergences, it appears interesting to restrict the dual (50) to \mathcal{H}_K and adding the regularizer $-\frac{\lambda}{2} \|\cdot\|_{\mathcal{H}_K}^2$, leading to

$$\tilde{D}_{f,\nu}^\lambda(\mu) := \max_{h \in \mathcal{H}_K} \left\{ \mathbb{E}_\mu[h] - (\tilde{D}_{f,\nu})^*(h) - \frac{\lambda}{2} \|h\|_{\mathcal{H}_K}^2 \right\}, \quad \mu \in \mathcal{P}(\mathbb{R}^d). \quad (52)$$

In contrast to the dual (22), there is no constraint on h . However, for every $h \in \mathcal{H}_K$, we have to solve (51) to obtain $(\tilde{D}_{f,\nu}^\lambda)^*(h)$. For discrete $\mu, \nu \in \mathcal{P}(\mathbb{R}^d)$, the objective (52) already appears in [68, Eq. (7)]. In the following subsection we further analyze this *tight* formulation of the MMD-regularized f -divergence.

B.1 Theory

First, to derive a primal formulation, we prove $\tilde{G}_{f,\nu} \in \Gamma_0(\mathcal{H}_K)$ for the extended functional $\tilde{G}_{f,\nu}$.

Lemma 25. *Let $f'_\infty = \infty$. Then the function*

$$\tilde{G}_{f,\nu}: \mathcal{H}_K \rightarrow [0, \infty], \quad h \mapsto \begin{cases} D_{f,\nu}(\mu), & \text{if } \exists \mu \in \mathcal{P}(\mathbb{R}^d) \text{ such that } h = m_\mu, \\ \infty, & \text{else,} \end{cases}$$

is lower semicontinuous. In particular, we have $\tilde{G}_{f,\nu} \in \Gamma_0(\mathcal{H}_K)$.

Proof. We follow the proof of Lemma 7. For $(h_n)_n \subset \mathcal{H}_K$ with $h_n \rightarrow h \in \mathcal{H}_K$, we need to show $\tilde{G}_{f,\nu}(h) \leq \liminf_{n \rightarrow \infty} \tilde{G}_{f,\nu}(h_n)$. If $\liminf_{n \rightarrow \infty} \tilde{G}_{f,\nu}(h_n) = +\infty$, we are done. For $\liminf_{n \rightarrow \infty} \tilde{G}_{f,\nu}(h_n) < +\infty$, we pass to a subsequence without renaming such that $\tilde{G}_{f,\nu}(h_n) < \infty$ for all $n \in \mathbb{N}$ that realizes the lim inf. Then, there exist $\mu_n \in \mathcal{P}(\mathbb{R}^d)$ with $m_{\mu_n} = h_n$.

Since $f'_\infty = \infty$ and $D_f(\mu_n | \nu) = \tilde{G}_{f,\nu}(h_n) < \infty$, we have $\mu_n \ll \nu$ for all $n \in \mathbb{N}$. Since f is an entropy function with $f'_\infty = \infty$, its conjugate f^* is continuous and strictly monotone on $(0, \infty) \subset \text{dom}(f^*)$ with $f^*(0) = 0$ and $f^*(t) \rightarrow \infty$ for $t \rightarrow \infty$ by [45, Sec. 2.3]. For the closed Euclidean ball $B_r \subset \mathbb{R}^d$ around 0 with radius r , we define

$$g: (0, \infty) \rightarrow [0, \infty], \quad r \mapsto \begin{cases} (f^*)^{-1}(\nu(\mathbb{R}^d \setminus B_r)^{-1}) & \text{if } \nu(B_r) \neq 1, \\ +\infty & \text{else.} \end{cases}$$

Due to [45, Eq. (2.20)] we have $\lim_{r \rightarrow \infty} g(r) = \infty$. The estimate becomes trivial when $\nu(B_r) = 1$, hence we assume $\nu(B_r) < 1$. For any $r > 0$, we estimate

$$\begin{aligned} \tilde{G}_{f,\nu}(h_n) &= \int_{\mathbb{R}^d} f \circ \frac{d\mu_n}{d\nu} d\nu \geq \int_{\mathbb{R}^d \setminus B_r} f \circ \frac{d\mu_n}{d\nu} - g(r) \frac{d\mu_n}{d\nu} d\nu + g(r) \mu_n(\mathbb{R}^d \setminus B_r) \\ &\geq \int_{\mathbb{R}^d \setminus B_r} -f^*(g(r)) d\nu + g(r) \mu_n(\mathbb{R}^d \setminus B_r) \geq -1 + g(r) \mu_n(\mathbb{R}^d \setminus B_r). \end{aligned}$$

Since $\liminf_{n \rightarrow \infty} \tilde{G}_{f,\nu}(h_n) < +\infty$, the sequence $(\tilde{G}_{f,\nu}(h_n))_n$ is bounded by some $B > 0$. To show that $(\mu_n)_n$ is tight, let $\varepsilon > 0$ and choose r large enough to satisfy $\frac{B+1}{\varepsilon} < g(r)$. Then, we can estimate with the convention $\frac{B+1}{\infty} = 0$ that

$$\varepsilon > \frac{B+1}{g(r)} \geq \frac{\tilde{G}_{f,\nu}(h_n) + 1}{g(r)} \geq \mu_n(\mathbb{R}^d \setminus B_r).$$

Hence, $(\mu_n)_n$ is tight and by [11, Thm. 5.1] it has a weakly convergent subsequence $\mu_{n_k} \rightarrow \mu \in \mathcal{P}(\mathbb{R}^d)$. Similarly to (18), we obtain $h = m_\mu$. Using Lemma 6, we get that $\tilde{G}_{f,\nu}$ is lower semicontinuous. Since $\mathcal{P}(\mathbb{R}^d)$ and $D_{f,\nu}$ are convex, we finally get $\tilde{G}_{f,\nu} \in \Gamma_0(\mathcal{H}_K)$. \square

Now, we can show that the primal formulation of $\tilde{D}_{f,\nu}^\lambda$ is like (14), but with feasible set $\mathcal{P}(\mathbb{R}^d)$ instead of $\mathcal{M}_+(\mathbb{R}^d)$.

Lemma 26 (Primal formulation of $\tilde{D}_{f,\nu}^\lambda$). *Assume that $f'_\infty = \infty$. Let $\lambda > 0$ and $\mu, \nu \in \mathcal{P}(\mathbb{R}^d)$. Then we have*

$$\tilde{D}_{f,\nu}^\lambda(\mu) = \min_{\sigma \in \mathcal{P}(\mathbb{R}^d)} \left\{ D_{f,\nu}(\sigma) + \frac{1}{2\lambda} d_K(\sigma, \nu)^2 \right\} \quad (53)$$

and the relationship with the maximizer in (52) is $m_{\hat{\sigma}} = m_\mu - \lambda \hat{h}$. Moreover, we have

$$\frac{\lambda}{2} \|\hat{h}\|_{\mathcal{H}_K}^2 \leq \tilde{D}_{f,\nu}(\mu) \leq \|\hat{h}\|_{\mathcal{H}_K} d_K(\mu, \nu). \quad (54)$$

Proof. We follow the proof of Corollary 10. The Moreau envelope $\tilde{G}_{f,\nu}^\lambda$ of $\tilde{G}_{f,\nu}$ is

$$\tilde{G}_{f,\nu}^\lambda(m_\mu) = \min_{\sigma \in \mathcal{P}(\mathbb{R}^d)} \left\{ \tilde{D}_{f,\nu}(\sigma) + \frac{1}{2\lambda} d_K(\sigma, \mu)^2 \right\}.$$

Moreover, for $p \in \mathcal{H}_K$, we have

$$(\tilde{G}_{f,\nu})^*(p) = \sup_{h \in \mathcal{H}_K} \langle p, h \rangle_{\mathcal{H}_K} - \tilde{G}_{f,\nu}(h) = \sup_{\mu \in \mathcal{P}(\mathbb{R}^d)} \langle p, \mu \rangle_{\mathcal{C}_0 \times \mathcal{M}} - \tilde{D}_{f,\nu}(\mu) = (\tilde{D}_{f,\nu})^*(p).$$

Hence, incorporating Theorem 1, $\tilde{G}_{\nu,f}$ can be written as

$$\begin{aligned} \tilde{G}_{f,\nu}^\lambda(m_\mu) &= \max_{p \in \mathcal{H}_K} \left\{ \mathbb{E}_\mu[p] - (\tilde{G}_{f,\nu})^*(p) - \frac{\lambda}{2} \|p\|_{\mathcal{H}_K}^2 \right\} \\ &= \max_{p \in \mathcal{H}_K} \left\{ \mathbb{E}_\mu[p] - (\tilde{D}_{f,\nu})^*(p) - \frac{\lambda}{2} \|p\|_{\mathcal{H}_K}^2 \right\} = \tilde{D}_{f,\nu}^\lambda(\mu). \end{aligned}$$

Both the relationship between the optimizers and the lower bound in (54) follow as in Corollary 10. For the upper bound, note that for $g \in \mathcal{H}_K$, we have

$$\tilde{G}_{f,\nu}^*(g) = \sup_{h \in \mathcal{H}_K} \langle g, h \rangle - \tilde{G}_{f,\nu}(h) \geq \langle g, m_\nu \rangle - \tilde{G}_{f,\nu}(m_\nu) = \mathbb{E}_\nu[g]$$

and thus

$$\tilde{D}_{f,\nu}^\lambda(\mu) = \mathbb{E}_\mu[\hat{h}] - (\tilde{G}_{f,\nu})(\hat{h}) - \frac{\lambda}{2} \|\hat{h}\|_{\mathcal{H}_K}^2 \leq \mathbb{E}_\mu[\hat{h}] - \mathbb{E}_\nu[\hat{h}] \leq \|\hat{h}\|_{\mathcal{H}_K} d_K(\mu, \nu).$$

□

The primal form (53) appears in [12, Thm. 6] for integral probability metrics instead of just MMDs. However, their restrictions on f are stronger than ours.

Remark 27 (Difference between tight and non-tight formulation). *The difference between $D_{f,\nu}^\lambda$ and $\tilde{D}_{f,\nu}^\lambda$ becomes obvious for $\nu = \delta_y$ with $y \in \mathbb{R}^d$ and $\mu = \delta_x$ with $x \in \mathbb{R}^d \setminus \{y\}$. If $f'_\infty = \infty$, then we have*

$$\tilde{D}_{f,\delta_y}^\lambda(\delta_x) = D_{f,\delta_y}(\delta_x) + \frac{1}{2\lambda} d_K(\delta_x, \delta_y) = \frac{1}{2\lambda} (K(x, x) + K(y, y) - 2K(x, y)),$$

whereas

$$D_{f,\delta_y}^\lambda(\delta_x) = \min_{a \geq 0} f(a) + \frac{1}{2\lambda} (a^2 K(y, y) + K(x, x) - 2aK(x, y)).$$

For the Tsallis-2 entropy function $f = f_2 = (\cdot - 1)^2$ we get

$$\arg \min_{a \geq 0} f(a) + \frac{1}{2\lambda} d_K(a\delta_x, \delta_y)^2 = \frac{2\lambda + K(x, y)}{2\lambda + K(y, y)}.$$

Since the radial kernel K is a decreasing function of the squared norm, the optimal $a^* = K(x, y)$ is in general smaller than 1. If, additionally we require that $K(x, x) = 1$ for all $x \in \mathbb{R}$, then we have the optimal value

$$D_{f, \delta_y}^\lambda(\delta_x) = \frac{1 - K(x, y)}{\lambda} \frac{K(x, y) + 4\lambda + 1}{2(2\lambda + 1)}.$$

The theoretical justification for the existence of Wasserstein gradient flows based on Theorem 15 uses Theorem 19 and Lemma 20, which only require the dual estimates (23) and not the dual (22) itself. Hence, the argumentation remains valid for the tight formulation (52). In Lemma 24, we showed that the dual representation (52) has a finite representation even for $f'_\infty < \infty$. Unfortunately, this result does not generalize straightforwardly.

B.2 Numerical Implementation Details

Following Section 5, we propose an Euler forward scheme for the Wasserstein-2 gradient flow of $\tilde{D}_{f, \nu}^\lambda$ for $\nu = \frac{1}{M} \sum_{j=1}^M \delta_{y_j}$ and $f'_\infty = \infty$. The primal problem (53) is finite-dimensional since $\sigma \in \mathcal{P}(\mathbb{R}^d)$ must be absolutely continuous with respect to ν . In particular, only M weights have to be optimized in (45) and $\hat{\sigma}_n(\mathbb{R}^d) = \sum_{k=1}^{M+N} \beta_k^{(n)} = 1$. Thus, we have $\beta_k^{(n)} = 0$, $k \in \{M+1, \dots, M+N\}$, i.e.,

$$b_k^{(n)} = \frac{1}{\lambda N}, \quad k = M+1, \dots, M+N, \quad \text{and} \quad \sum_{k=1}^M b_k^{(n)} = -\frac{1}{\lambda}. \quad (55)$$

This can be reformulated as

$$q_{M+j}^{(n)} = -\frac{M}{N}, \quad j = 1, \dots, N, \quad q_k^{(n)} \geq 0, \quad k = 1, \dots, M, \quad \text{and} \quad \sum_{k=1}^M q_k^{(n)} = M. \quad (56)$$

This means that $\frac{1}{M} (q_k^{(n)})_{k=1}^M$ is an element of the unit simplex in \mathbb{R}^M . We minimize the objective J from (47) subject to (56) with exponentiated gradient descent, that is, mirror descent where the mirror map is the negative Shannon entropy. We use an Armijo line search or Polyak rule [87, Algorithm 3] for determining the step size in each iteration, which leads to convergence if J is differentiable [44]. Both approaches only require one gradient per iteration. The advantage of the Polyak step size is that it also only requires one function evaluation. Mirror descent works relatively well in high dimension [8] and is parallelizable on the GPU. In our simulations, the gradient flow for $\tilde{D}_{f, \nu}^\lambda$ tends to stay closer to the target and has a lower number of outliers; see Figure 8. Although the differences are most pronounced for the bananas target, a similar effect occurs for the others.

Remark 28 (Tractability of FISTA for the primal problem). *The separability of $\text{prox}_{\tilde{h}_1}$ is lost when we restrict the minimization of J to the simplex. Hence, it is unclear if FISTA would be effective when applied to (49). Due to (55), the same problem would also occur for the dual objective.*

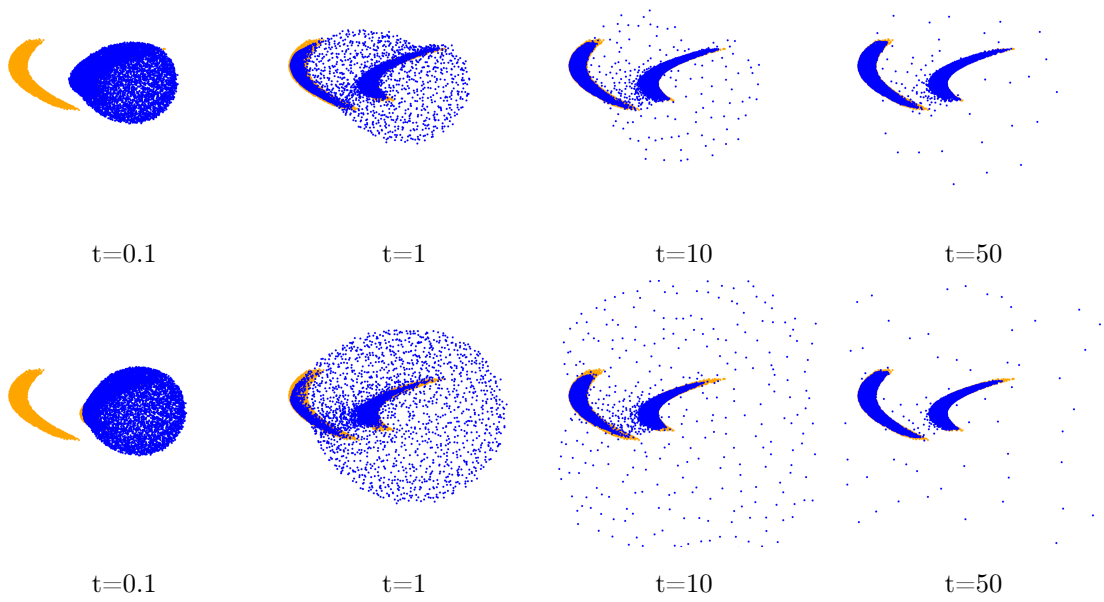


Figure 8: WGF of the tight version $\tilde{D}_{f,\nu}^\lambda$ (top) and non-tight one $D_{f,\nu}^\lambda$ (bottom) of the regularized Tsallis-2 divergence for the bananas target and $N = M = 9000$.

C Duality gaps and optimality criteria

Here, we collect some details about tracking the accuracy of the numerical solvers for the dual problem and when to terminate the iterations. The duality gap is the difference between the dual optimal value and the primal optimal value, namely

$$\text{dg}^{(n)} := \left| -D(\hat{b}^n) - J(q^{(n)}) \right|.$$

Since we only minimize J , we instead calculate the primal pseudo-duality gap

$$\text{dg}_p^{(n)} := \left| -D\left(-\frac{1}{\lambda M}q^{(n)}\right) - J(q^{(n)}) \right|.$$

To account for small functional values towards the end of the iteration, we can replace this with its relative counterpart, where we divide by the minimum of the two summands. When computing the particle flows, we terminate the time stepping if the “kinetic energy” $-\partial_t D_{f,\nu}^\lambda(\gamma_n) = \frac{1}{N} \sum_{i=1}^N |\nabla p_n(x_i^{(n)})|^2$ is small.

D Supplementary Material

Here, we provide more numerical experiments and give some implementation details.

D.1 Implementation Details

To leverage parallel computing on the GPU, we implemented our model in PyTorch [57]. Furthermore, we use the Scikit-learn package [59] for the generation of some target measures ν , the Matplotlib package [34] for figures and the POT package [69] for calculating $W_2(\mu, \nu)^2$ along the flow. Solving the dual (43) turned out to be much more time-consuming than solving the primal problem (21), so we exclusively outlined the implementation for the latter. As a sanity check, we calculate the “pseudo-duality gap”, which is the difference between the value of the primal objective at the solution q and the value of the dual objective at the corresponding dual certificate $\frac{1}{\lambda N}[-q, \mathbf{1}_N]$. Then, the relative pseudo-duality gap is computed as the quotient of the pseudo-duality gap and the minimum of the absolute value of the involved objective values. Since the particles get close to the target towards the end of the flow, we use double precision throughout (although this deteriorates the benefit of GPUs). With this, all quantities can still be accurately computed and evaluated.

D.2 The Kernel Width

For the first ablation study, we use the parameters from Section 6, namely $\alpha = 5$, $\lambda = 10^{-2}$, $\tau = 10^{-3}$ and $N = 900$. In Figure 9, we see that the kernel width has to be calibrated carefully to get a sensible result. We observe that the width $\sigma^2 = 10^{-3}$ is too small. In particular, the repulsion of the particles is too powerful, and they immediately spread out

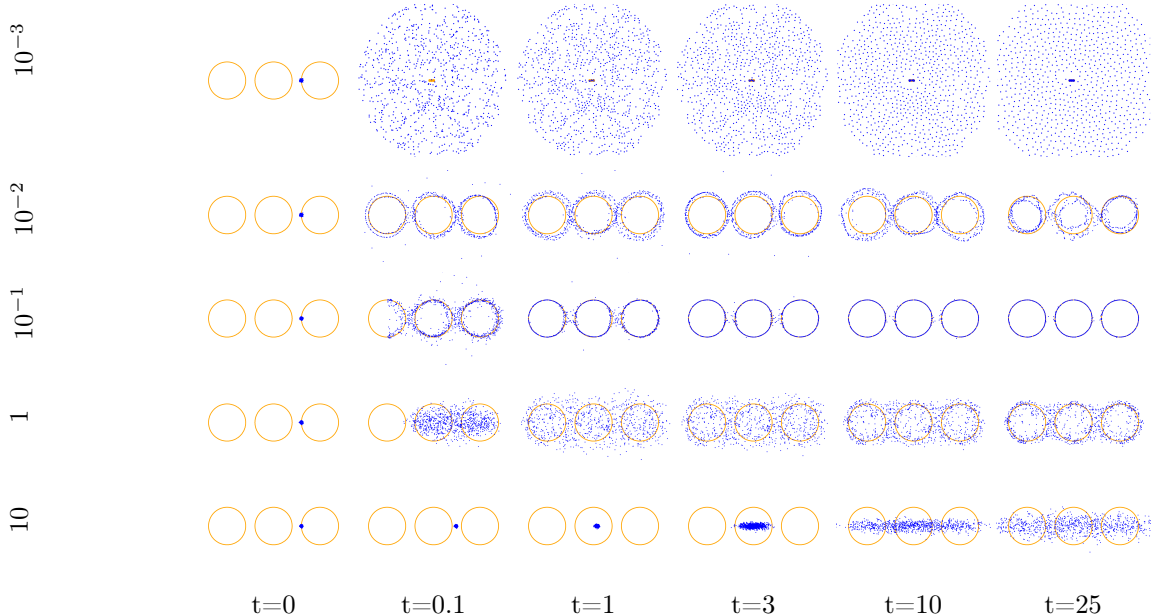


Figure 9: Ablation study for the parameter σ^2 of the inverse multiquadric kernel.

before moving towards the rings, but only very slowly. If $\sigma^2 = 10^{-2}$, everything works out reasonably, and there are no outliers. For $\sigma^2 = 10$, the particles only recover the support of the target very loosely.

The Matern kernel with smoothness parameter $\nu = \frac{3}{2}$, see [64, Subsec. 4.2.1], reads

$$k_{\sigma^2, \frac{3}{2}}(x, y) = \left(1 + \frac{\sqrt{3}}{\sigma^2} \|x - y\|_2\right) \exp\left(-\frac{\sqrt{3}}{\sigma^2} \|x - y\|_2\right),$$

The shape of the flow for different kernel widths σ^2 is quite different. In Figure 10, we choose $\alpha = 3$, $\lambda = 10^{-2}$, $\tau = 10^{-3}$ and $N = 900$. We can see that when the width $\sigma^2 = 10^{-3}$ is too small, then the particles barely move. The particles only spread on the two rightmost rings for $\sigma^2 = 10^{-2}$. For $\sigma^2 = 10^{-1}$, the particles initially spread only onto two rings but also match the third one after some time. The width $\sigma^2 = 1$ performs best, and there are no outliers. For $\sigma^2 = 10$, the behavior is very similar to the case $\sigma^2 = 10$ in Figure 9. For $\sigma^2 = 10^2$, we observe an extreme case of mode-seeking behavior: the particles do not spread and only move towards the mean of the target distribution.

D.3 The Regularization Parameter λ

First, we investigate the behavior of the flow if only the regularization parameter λ varies. For this purpose, we choose the Jeffreys divergence. In our scheme, we choose $\tau = 10^{-3}$

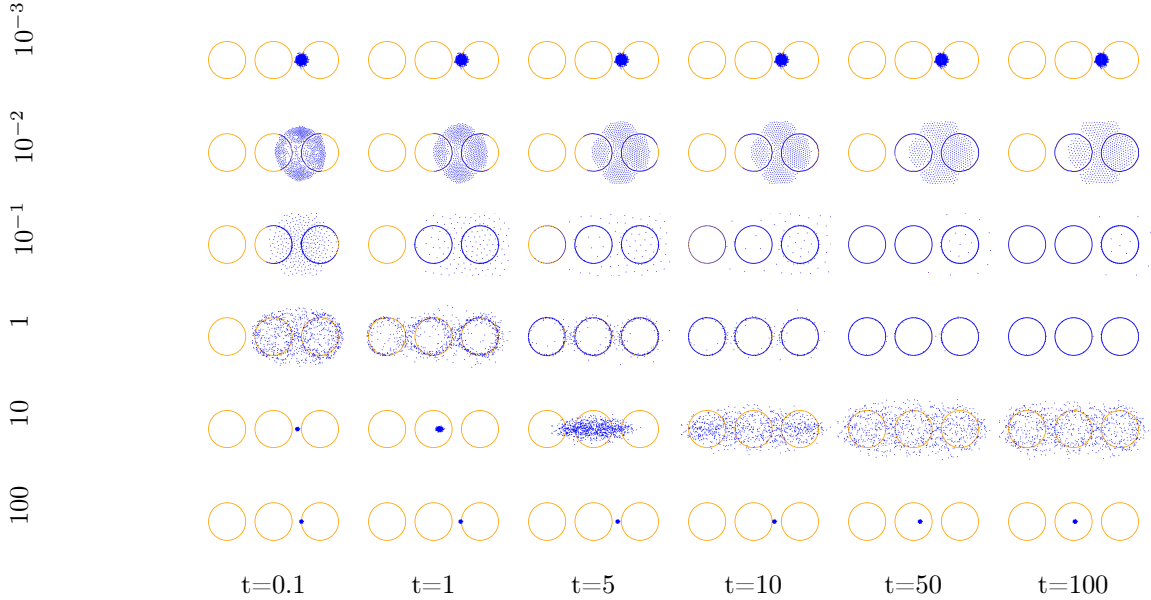


Figure 10: Ablation study for the parameter σ^2 of the Matern kernel with $\nu = \frac{3}{2}$.

and $N = 900$ and the inverse multiquadric kernel with width $\sigma^2 = 5 \times 10^{-1}$. Even though the Jeffreys entropy function is infinite at $x = 0$, the flow still behaves reasonably well, see Figure 11. If λ is very small, many particles get stuck in the middle and do not spread towards the funnels. If, however, λ is much larger than the step size τ , then the particles only spread out slowly and in a spherical shape. This behavior is also reflected in the corresponding distances to the target measure ν , see Figure 12. In our second example, we use the compactly supported “spline” kernel $k(x, y) := (1 - \|x - y\|_2)_+^3 (3\|x - y\| + 1)$, the 3-Tsallis divergence, $\tau = 10^{-3}$, $N = 900$ and the three circles target from before, see Figure 13. Overall, the behavior is similar to before.

To find the combinations of λ and τ that give the best results, we use the two “two bananas” target and evaluate each flow after 100 iterations of the forward Euler scheme. Note that $\frac{\tau}{\lambda}$ is the prefactor in front of the gradient term in the update step (48). Hence, it influences how much gradient information is taken into consideration when updating the particles. The results are provided in Figure 14. We observed that the behavior for $\lambda \in \{10^2, 10^3\}$ is nearly identical to the behavior for $\lambda = 10$.

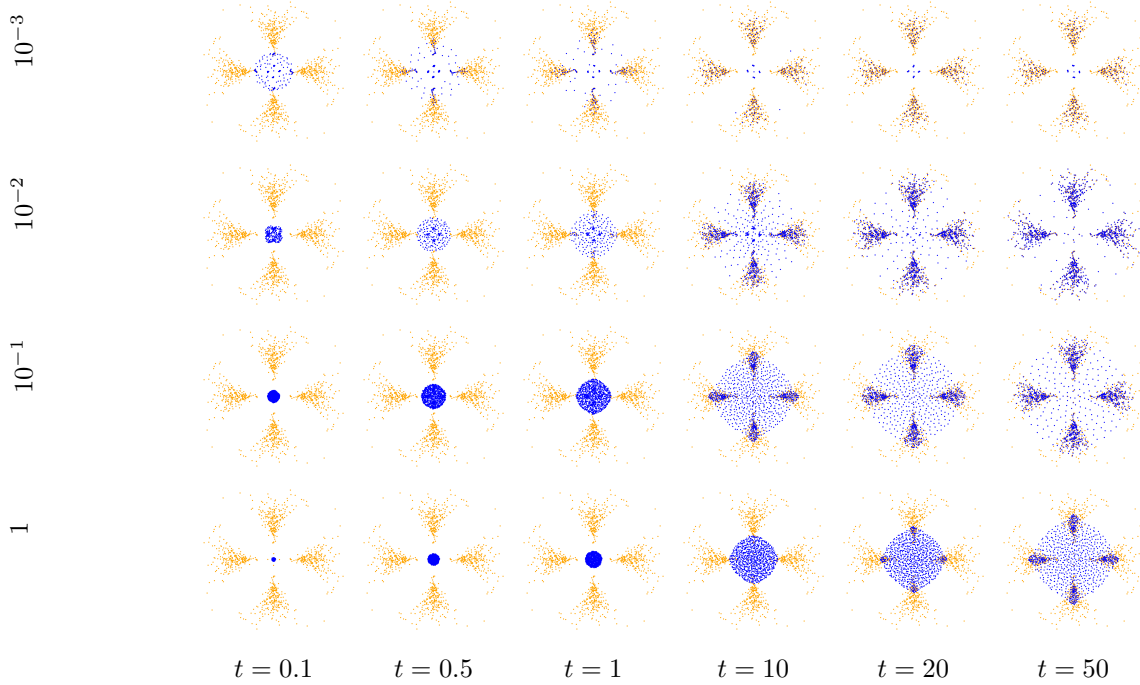


Figure 11: Ablation study for the parameter λ , illustrated for the Jeffreys divergence.

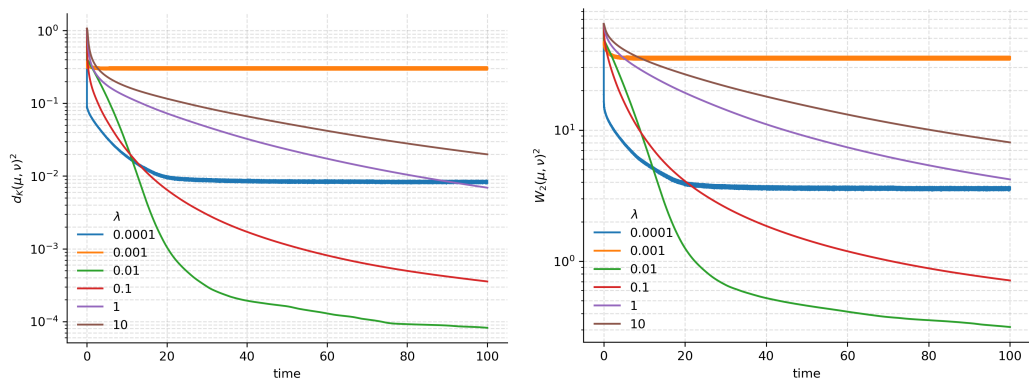


Figure 12: Comparison of the squared MMD (**left**) and W_2 distance (**right**) for Figure 11.

Table 2: The f -divergences belonging to the entropy functions from Table 1.

divergence D_f	$D_f(\mu \mid \nu)$, where $\mu = \rho\nu + \mu^s$
Tsallis- α , $\alpha \in (0, 1)$	$\frac{1}{\alpha-1} \left[\int_{\mathbb{R}^d} \rho(x)^\alpha - 1 \, d\nu(x) - \alpha(\mu(\mathbb{R}^d) - \nu(\mathbb{R}^d)) \right]$
Tsallis- α , $\alpha > 1$	$\begin{cases} \frac{1}{\alpha-1} \left[\int_{\mathbb{R}^d} \rho(x)^\alpha - 1 \, d\nu(x) - \alpha(\mu(\mathbb{R}^d) - \nu(\mathbb{R}^d)) \right], & \text{if } \mu^s = 0, \\ \infty, & \text{else.} \end{cases}$
power divergence, $\alpha < 1, \alpha \neq 0$	$\int_{\mathbb{R}^d} \frac{\rho(x)^{\alpha-1}}{\alpha(\alpha-1)} \, d\nu(x) + \frac{1}{\alpha-1} (\nu(\mathbb{R}^d) - \mu(\mathbb{R}^d))$
power divergence, $\alpha > 1$	$\begin{cases} \int_{\mathbb{R}^d} \frac{\rho(x)^{\alpha-1}}{\alpha(\alpha-1)} \, d\nu(x) + \frac{1}{\alpha-1} (\nu(\mathbb{R}^d) - \mu(\mathbb{R}^d)), & \text{if } \mu^s = 0, \\ \infty, & \text{else.} \end{cases}$
Kullback-Leibler	$\begin{cases} \int_{\mathbb{R}^d} \rho(x) \ln(\rho(x)) \, d\nu(x) - \mu(\mathbb{R}^d) + \nu(\mathbb{R}^d) & \text{if } \mu^s = 0, \\ \infty & \text{else.} \end{cases}$
Jeffreys	$\begin{cases} \int_{\mathbb{R}^d} (\rho(x) - 1) \ln(\rho(x)) \, d\nu(x), & \text{if } \mu^s = 0 \text{ and } \nu(\{\rho = 0\}) = 0, \\ \infty, & \text{else} \end{cases}$
Vajda's χ^α , $\alpha > 1$	$\begin{cases} \int_{\mathbb{R}^d} \rho(x) - 1 ^\alpha \, d\nu(x), & \text{if } \mu^s = 0, \\ \infty, & \text{else.} \end{cases}$
equality indicator	$\begin{cases} 0 & \text{if } \mu = \nu, \\ \infty & \text{otherwise} \end{cases}$
Jensen-Shannon	$\int_{\mathbb{R}^d} \rho(x) \ln(\rho(x)) - (\rho(x) + 1) \ln\left(\frac{1}{2}(\rho(x) + 1)\right) \, d\nu(x) + \ln(2)\mu^s(\mathbb{R}^d)$
α -Lindsay, $\alpha \in [0, 1)$	$\int_{\mathbb{R}^d} \frac{(\rho(x)-1)^2}{\alpha+(1-\alpha)\rho(x)} \, d\nu(x) + \frac{1}{1-\alpha}\mu^s(\mathbb{R}^d)$
Perimeter-type, $\alpha \in \mathbb{R} \setminus \{0, 1\}$	$\frac{\operatorname{sgn}(\alpha)}{1-\alpha} \left[\int_{\mathbb{R}^d} \left(\rho(x)^{\frac{1}{\alpha}} + 1 \right)^\alpha \, d\nu(x) - 2^{\alpha-1} (\mu(\mathbb{R}^d) + \nu(\mathbb{R}^d)) + \mathbb{1}_{(0, \infty)}(\alpha) \mu^s(\mathbb{R}^d) \right]$
Burg	$\begin{cases} \int_{\mathbb{R}^d} \ln(\rho(x)) \, d\nu(x) + \mu(\mathbb{R}^d) - \nu(\mathbb{R}^d), & \text{if } \nu(\{\rho = 0\}) = 0, \\ \infty, & \text{else.} \end{cases}$
Symmetrized Tsallis	$\mu(\mathbb{R}^d) + \nu(\mathbb{R}^d) - \int_{\mathbb{R}^d} \rho(x)^s + \rho(x)^{1-s} \, d\nu(x)$
Matusita	$\int_{\mathbb{R}^d} 1 - \rho(x) ^{\frac{1}{\alpha}} \, d\nu(x) + \mu^s(\mathbb{R}^d)$
Kafka	$\int_{\mathbb{R}^d} 1 - \rho(x) ^\alpha (1 + \rho(x))^{\frac{\alpha-1}{\alpha}} \, d\nu(x) + \mu^s(\mathbb{R}^d)$
total variation	$\int_{\mathbb{R}^d} \rho(x) - 1 \, d\nu(x) + \mu^s(\mathbb{R}^d)$
Marton	$\frac{1}{2} \int_{\mathbb{R}^d} \rho(x) - 1 \, d\nu(x) + \frac{1}{2} (\nu(\mathbb{R}^d) - \mu(\mathbb{R}^d))$
Hockey stick	$\int_{\mathbb{R}^d} (1 - \rho(x))_+ \, d\nu(x)$
zero	0

f	$\text{prox}_{\lambda f}(x)$
f_{KL}	$\lambda W\left(\frac{1}{\lambda} \exp\left(\frac{x}{\lambda}\right)\right)$
Tsallis-2	$\frac{1}{2\lambda+1}(2\lambda+x)_+$
Burg	$\frac{1}{2}\left(x-\lambda+\sqrt{(x-\lambda)^2+4\lambda}\right)$
TV	$\begin{cases} S_\lambda(x-\lambda), & \text{if } x \geq -\lambda, \\ 0, & \text{else.} \end{cases}$
Marton	$\begin{cases} \frac{1}{1+2\lambda}(x+2\lambda)_+, & \text{if } x \leq 1, \\ x, & \text{else.} \end{cases}$
equality indicator	1
zero	$(x)_+$

Table 3: Closed forms for proximal operators of some entropy functions. Here, $\lambda > 0$, S_λ denotes the soft-shrinkage operator, W is the (principal branch of the) Lambert-W function [21], and $(\cdot)_+$ the non-negative part of a real number.

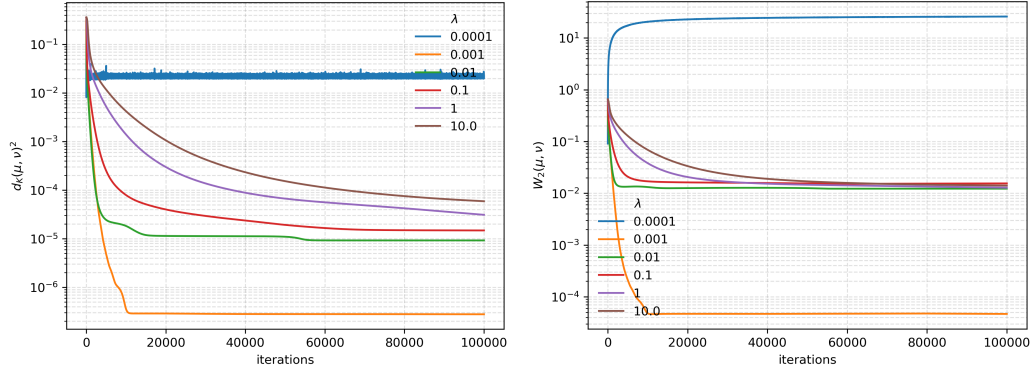


Figure 13: Comparing the squared MMD (**left**) and W_2 distance (**right**) for different λ .

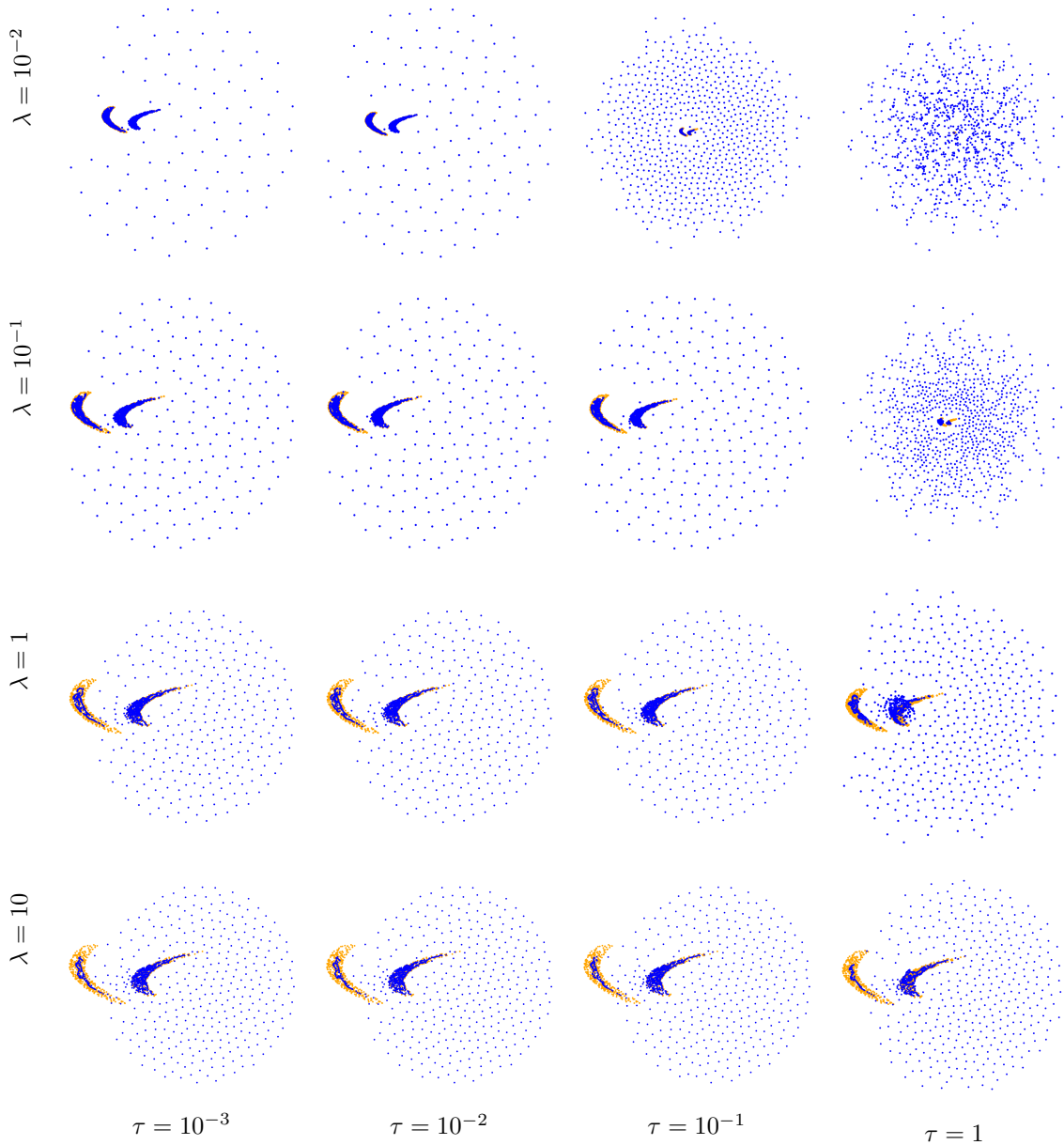


Figure 14: Here, we use $\alpha = 2$, the inverse multiquadric kernel with width $\sigma^2 = 5 \times 10^{-2}$, and $N = 900$. We plot the configuration of the particles at $t = 100$. One should not choose τ to be larger than λ by orders of magnitude.